

See discussions, stats, and author profiles for this publication at: <https://www.researchgate.net/publication/231681207>

Scanning Tunneling Microscopy Investigation of the Ordered Structures of Dialkylamino Hydroxylated Squaraines Adsorbed on Highly Oriented Pyrolytic Graphite

ARTICLE *in* LANGMUIR · FEBRUARY 2000

Impact Factor: 4.46 · DOI: 10.1021/la990210t

CITATIONS

47

READS

7

3 AUTHORS, INCLUDING:



Bruce A Parkinson

University of Wyoming

251 PUBLICATIONS 6,953 CITATIONS

SEE PROFILE

Scanning Tunneling Microscopy Investigation of the Ordered Structures of Dialkylamino Hydroxylated Squaraines Adsorbed on Highly Oriented Pyrolytic Graphite

M. E. Stawasz, D. L. Sampson,[†] and B. A. Parkinson*

Department of Chemistry, Colorado State University, Fort Collins, Colorado 80523

Received February 23, 1999. In Final Form: July 30, 1999

Squaraine dyes form aggregates in solution and in the solid state. We have found that squaraines form two-dimensional (2D) ordered layers when adsorbed onto HOPG from phenyloctane and from liquid crystalline solvents. We investigated with scanning tunneling microscopy the 2D structures of the adsorbed phases of five bis(4-alkylamino-2-hydroxyphenyl) squaraines (both symmetric and asymmetric) and mixtures of these squaraines. Differences in the stability of the 2D structures and molecular packing are observed when the alkyl tail length and symmetry are varied. A transition in the 2D structure from a herringbone packing to a lamellar packing occurs between the tail lengths of 4 carbons and 8 carbons. Many of the compounds form a number of 2D polytypes on HOPG. Multilayers of squaraine molecules were observed for most of the studied molecules. Squaraines with tail lengths of 12 carbons exhibited a tendency toward registry with the HOPG substrate whereas all other squaraine compounds investigated showed a lack of molecule–substrate registry. Domain sizes of the investigated molecules varied from tens of nanometers to a micron.

Introduction

Since the invention of scanning tunneling microscopy (STM), a number of different organic molecular systems that form two-dimensional (2D) ordered arrays on solid surfaces have been studied. These systems can be roughly divided into three basic types distinguished from each other by the relative strengths of their molecule–molecule and molecule–substrate interactions. The first type, represented by alkanes and alkane derivatives on HOPG, exhibits only weak van der Waals molecule–molecule interactions.^{1–18} Although there are molecule–molecule interactions, the two-dimensional organization of molecules within this type of molecular system is primarily driven by interaction between the adsorbed molecules and the substrate. Changing the lattice spacing of the substrate

changes the relationship of the molecules within the adsorbate layer, often resulting in little or no two-dimensional order.

The second group shows a relatively balanced influence of intermolecular interactions within the adsorbed layer and between the adsorbed molecules and the substrate. This system is best exemplified by liquid crystals.^{19–34} Molecules that form liquid crystalline phases generally contain a polar head group and an aliphatic tail. Within the adsorbate layer the main intermolecular interactions are dipole–dipole and van der Waals. Between the adsorbate layer and the substrate, the interaction tends to be driven by alkyl tail registry with the substrate lattice. Both the adsorbate–adsorbate and adsorbate–substrate interactions exert an influence on the two-dimensional

[†] Current address: Digital Instruments, San Jose, CA.

- (1) McGonigal, G. C.; Bernhardt, R. H.; Thomson, D. J. *Appl. Phys. Lett.* **1990**, *57*, 28–30.
- (2) Thibaudau, F.; Watel, G.; Cousty, J. *Surf. Sci. Lett.* **1993**, *281*, L303–L307.
- (3) Watel, G.; Thibaudau, F.; Cousty, J. *Surf. Sci. Lett.* **1993**, *281*, L297–L302.
- (4) Wawkuschewski, A.; Cantow, H.-J.; Magonov, S. N. *Langmuir* **1993**, *9*, 2778–2781.
- (5) Askadskaya, L.; Rabe, J. P. *Phys. Rev. Lett.* **1992**, *69*, 1395–1398.
- (6) Cincotti, S.; Rabe, J. P. *Supramol. Sci.* **1994**, *1*, 7–10.
- (7) Claypool, C. L.; Faglioni, F.; Goddard, W. A., III; Gray, H. B.; Lewis, N. S.; Marcus, R. A. *J. Phys. Chem. B* **1997**, *101*, 5978–5995.
- (8) Giancarlo, L.; Cyr, D.; Muyskens, K.; Flynn, G. W. *Langmuir* **1998**, *14*, 1465–1471.
- (9) Groszek, A. J. *Proc. R. Soc. London A* **1970**, *314*, 473–498.
- (10) Habenschuss, A.; Narten, A. H. *J. Chem. Phys.* **1990**, *92*, 5692–5699.
- (11) Peters, G. H. *Surf. Sci.* **1996**, *347*, 169–181.
- (12) Rabe, J. P.; Buchholtz, S. *Science* **1991**, *253*, 424–427.
- (13) Rabe, J. P.; Buchholz, S.; Askadskaya, L. *Phys. Scr.* **1993**, *T49*, 260–263.
- (14) Segerman, E. *Acta Crystallographica* **1965**, *19*, 789–796.
- (15) Venkataraman, B.; Breen, J. J.; Flynn, G. W. *J. Phys. Chem.* **1995**, *99*, 6608–6619.
- (16) Cyr, D. M.; Venkataraman, B.; Flynn, G. W. *Chem. Mater.* **1996**, *8*, 1600–1615.
- (17) Hentschke, R.; Schurmann, B. L.; Rabe, J. P. *J. Chem. Phys.* **1992**, *96*, 6213.
- (18) Cincotti, S.; Rabe, J. P. *Appl. Phys. Lett.* **1993**, *62*, 3531.

- (19) Stevens, F.; Dyer, D. J.; Walba, D. M. *Langmuir* **1996**, *12*, 436–440.
- (20) Stevens, F.; Dyer, D. J.; Walba, D. M.; Shao, R.; Clark, N. A. *Liq. Cryst.* **1997**, *22*, 531–534.
- (21) Palermo, V.; Biscarini, F.; Zannoni, C. *Phys. Rev. E* **1998**, *57*, R2519–R2522.
- (22) Stevens, F.; Patrick, D. L.; Cee, V. J.; Purcell, T. J.; Beebe, T. P., Jr. *Langmuir* **1998**, *14*, 2396–2401.
- (23) Spong, J. K.; Mizes, H. A.; LaComb, J.; Dovek, M. M.; Frommer, J. E.; Foster, J. S. *Nature* **1989**, *338*, 137–139.
- (24) Patrick, D. L.; Cee, V. J.; Purcell, T. J.; Beebe, T. P., Jr. *Langmuir* **1996**, *12*, 1830–1835.
- (25) Patrick, D. L.; Cee, V. J.; Beebe, T. P., Jr. *Science* **1994**, *265*, 231–234.
- (26) Cleaver, D. J.; Callaway, M. J.; Forester, T.; Smith, W.; Tildesley, D. J. *Mol. Phys.* **1995**, *86*, 613–636.
- (27) Smith, D. P. E.; Heckl, W. M.; Klagges, H. A. *Surf. Sci.* **1992**, *278*, 166–174.
- (28) Lacaze, E.; Barois, P.; Lacaze, R. *J. Phys. I* **1997**, *7*, 1645–1664.
- (29) Smith, D. P. E.; Horber, H.; Gerber, C.; Binnig, G. *Science* **1989**, *245*, R43–R45.
- (30) Hara, M.; Iwakabe, Y.; Tochigi, K.; Sasabe, H.; Garito, A. F.; Yamada, A. *Nature* **1990**, *244*, 228–230.
- (31) Smith, D. P. E.; Horber, J. K. H.; Binnig, G.; Nejjoh, H. *Nature* **1990**, *244*, 641.
- (32) Iwakabe, Y.; Hara, M.; Kondo, K.; Oh-Hara, S.; Mukoh, A.; Sasabe, H. *Jpn. J. Appl. Phys.* **1992**, *31*, L1771–L1774.
- (33) Smith, D. P. E. *J. Vac. Sci. Technol. B* **1991**, *9*, 1119–1125.
- (34) Patrick, D. L.; Cee, V. J.; Beebe, T. P., Jr. *J. Phys. Chem.* **1996**, *100*, 8478–8481.

structure of the adsorbate layer. Thus, subtle changes in the substrate lattice constant or molecular structure can result in very different two-dimensional surface structures.³⁵

The third system of molecules, which spontaneously form 2D ordered arrays/layers on surfaces, are those in which adsorbate–adsorbate intermolecular interactions dominate the two-dimensional structure. Adenine molecules are indicative of this third type of adsorbate system.^{36–42} The relatively stronger hydrogen bonding between adjacent molecules controls the molecular packing of adenines and similar molecules in the adsorbed layer. When the lattice spacing of the substrate is changed, the packing order and distance relationship between adjacent adenine molecules within the layer do not change substantially.^{37–39,41}

We report a new ordered molecular adsorbate system, squaraine dye molecules (see Table 1 for structure), belonging to the third class described above. Squaraines are dyes so named because of the square central carbon ring.⁴³ They are highly polarized and symmetric molecules that are able to undergo intermolecular charge transfer in the ground state as well as in the first excited state. In the ground state the anilino moieties act as electron donors (D) while the central C₄O₂ unit acts as the electron acceptor (A), resulting in the squaraine molecule having a donor–acceptor–donor (DAD) internal structure. The DAD structure results in strongly attractive intermolecular interactions between the donor and acceptor moieties of adjacent molecules.^{44–48} In addition, its DAD structure makes the squaraine molecule a good charge-transfer vehicle, both intramolecularly and intermolecularly. Squaraines are strongly absorbing with extinction coefficients on the order of $3 \times 10^5 \text{ M}^{-1} \text{ cm}^{-1}$ in many solvents.⁴⁷ At low concentrations ($<10^{-6} \text{ M}$) in solution most squaraines exist as monomers, with λ_{max} varying between 627 and 661 nm, depending on the nitrogen and phenyl substituents.⁴⁹ At higher concentrations, however, aggregation of squaraines in solution is evident with λ_{max} shifted to the red or blue depending on the aggregate structure. The predominant industrial use for squaraines has been in photoreceptor devices as photogenerating molecules in xerography^{50,51} and ablative optical re-

cording,^{52–54} although they have also been used for research on organic solar cells.^{48,55–57}

The strong intermolecular interactions, resulting in a tendency to aggregate in solution, combined with intermolecular charge transfer make squaraines promising molecular systems for STM study. There is an additional applied justification for studying squaraine structures with STM. It has been shown that the three-dimensional structure of squaraines affects their ability to generate and transport charge in photoreceptor devices.⁴⁵ It has also been shown that *n*-alkyl substituents disturb the intermolecular CT interaction between the squaraine chromophores due to their steric bulk.⁵⁸ STM is useful for imaging the two-dimensional ordered structures of organic molecules on solid substrates. The goal of this study was to determine the effect of structural differences in the squaraine molecules on the two-dimensional packing structures formed on HOPG surfaces. This systematic variation in structure from short alkane chains to long alkane chains should also lead to a progression in adsorbate structure dominated by molecule–molecule interactions to structures showing a more balanced influence between molecule–molecule interactions and substrate–molecule interactions.

Experimental Section

Experiments were performed with a Digital Instruments Nanoscope III scanning tunneling microscope under ambient conditions. Vibration isolation was provided by a bungee system enclosed in an environmental chamber. Three different squaraine molecules were obtained from Dr. P. M. Kazmaier of the Xerox Research Centre of Canada. They were bis(4-dibutylamino-2-hydroxyphenyl) squaraine [4–4 SQ], bis(4-dioctylamino-2-hydroxyphenyl) squaraine [8–8 SQ], and bis(4-didodecylamino-2-hydroxyphenyl) squaraine [12–12]. Bis(4-ethylstearyl-amino-2-hydroxyphenyl) squaraine [2–18] was purchased from Nippon Kankoh-Shikiso Kenkyusho, and bis(4-(dimethylamino)-2-hydroxyphenyl) squaraine was provided by Dr. Gregg Haggquist of Lexmark. 4'-*n*-octyl-4-cyanobiphenyl (8CB) was obtained from Aldrich. Table 1 shows the structures of the five squaraine molecules studied and the abbreviations used in the rest of this paper. For single-component solutions, concentrations of approximately 10^{-4} to 10^{-6} M were prepared in phenyloctane (Aldrich). For binary squaraine solutions, mole percent ratios of 1:1, 1:10, and 10:1 were prepared. Mixtures of 2–18 SQ and 8CB were prepared by dissolving 0.1–5% wt/wt 2–18 SQ into neat 8CB. STM tips were cut to a sharp point mechanically from (80:20) platinum/iridium 0.2 mm diameter wire (Alpha Aesar). Samples were prepared by applying a drop of squaraine solution onto a freshly cleaved piece of highly ordered pyrolytic graphite (HOPG). Tunneling occurred with the tip immersed into the layer of solution using typical tunneling parameters of -2.0 to -1.6 V (sample negative) and 40 pA with the scanning

(35) Iwakabe, Y.; Hara, M.; Kondo, K.; Tochigi, K.; Mukoh, M.; Yamada, A.; Carito, A. F.; Sasabe, H. *Jpn. J. Appl. Phys.* **1991**, *30*, 2542.

(36) Allen, M. J.; Balooch, M.; Subbiah, S.; Tench, R. J.; Balhorn, R.; Siekhaus, W. *Ultramicroscopy* **1992**, *42–44*, 1049–1053.

(37) Tanaka, H.; Yoshinobu, J.; Kawai, M. *Jpn. J. Appl. Phys., Part 2* **1996**, *35*, L244–L246.

(38) Kasaya, M.; Tabata, H.; Kawai, T. *Surf. Sci.* **1996**, *357–358*, 195–201.

(39) Furukawa, M.; Tanaka, H.; Kawai, T. *Surf. Sci.* **1997**, *392*, L33–L39.

(40) Freund, J. E.; Edelwirth, M.; Krob, P.; Heckl, W. M. *Phys. Rev. B* **1997**, *55*, 5394–5397.

(41) Kawai, T.; Tanaka, H.; Nakagawa, T. *Surf. Sci.* **1997**, *386*, 124–136.

(42) Sowerby, S. J.; Edelwirth, M.; Reiter, M.; Heckl, W. M. *Langmuir* **1998**, *14*, 5195–5202.

(43) Schmidt, A. H. In *Oxocarbons*; West, R., Ed.; Academic Press: New York, 1980; p 185.

(44) Bigelow, R. W.; Freund, H. J. *Chem. Phys.* **1986**, *107*, 159–174.

(45) Law, K. Y. *Chem. Rev.* **1993**, *93*, 449–486.

(46) Tristani-Kendra, M.; Eckhardt, C. J.; Bernstein, J.; Goldstein, E. *Chem. Phys. Lett.* **1983**, *98*, 57.

(47) Tristani-Kendra, M.; Eckhardt, C. J. *J. Chem. Phys.* **1984**, *81*, 1160.

(48) Loutfy, R. O.; Hsiao, C. K.; Kazmaier, P. M. *Photogr. Sci. Eng.* **1983**, *27*, 5.

(49) Law, K. Y. *J. Phys. Chem.* **1987**, *91*, 5184–5193.

(50) Law, K. Y.; Bailey, F. C. *J. Imaging Sci.* **1987**, *31*, 83.

(51) Melz, R. J.; Champ, R. B.; Chang, L. S.; Chiou, C.; Keller, G. S.; Licican, L. C.; Neiman, R. B.; Shattuck, M. D.; Weihe, W. J. *Photogr. Sci. Eng.* **1977**, *21*, 73.

(52) Gravestijn, D. J.; Steenbergen, C.; Veen, J. v. d. *Proc. SPIE* **1983**, *420*, 327.

(53) Jipson, V. B.; Jones, C. R. *J. Vac. Sci. Technol.* **1981**, *18*, 105–109.

(54) Jipson, V. P.; Jones, C. R. *IBM Technol. Discl. Bull.* **1981**, *24*, 298.

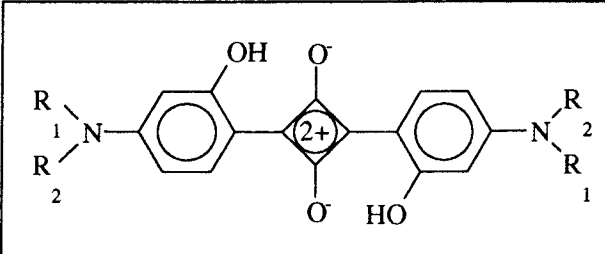
(55) Morel, D. L.; Stogryn, E. L.; Ghosh, A. K.; Feng, T.; Purwin, P. E.; Shaw, R. F.; Fishman, C.; Bird, G. R.; Piechowski, A. P. *J. Phys. Chem.* **1984**, *88*, 923.

(56) Piechowski, A. P.; Bird, G. R.; Morel, D. L.; Stogryn, E. L. *J. Phys. Chem.* **1984**, *88*, 934–950.

(57) Merritt, V. Y.; Hovel, H. J. *Appl. Phys. Lett.* **1976**, *29*, 414.

(58) Law, K. Y.; Facci, J. S.; Bailey, F. C.; Yanus, J. F. *J. Imaging Sci.* **1990**, *34*, 31.

Table 1. Structure of a Generic Squaraine Molecule and List of the Squaraines Studied

	
1-1 SQ	$R_1 = R_2 = C_1H_3$
4-4 SQ	$R_1 = R_2 = C_4H_9$
8-8 SQ	$R_1 = R_2 = C_8H_{17}$
12-12 SQ	$R_1 = R_2 = C_{12}H_{25}$
2-18 SQ	$R_1 = C_2H_5$ $R_2 = C_{18}H_{37}$

tunneling microscope operating in the constant current mode. After a series of squaraine images were obtained, the tunneling gap resistance was lowered in order to characterize the HOPG surface in the exact same spot. Images were obtained with different tips and several different series of solutions to test for reproducibility and ensure that data were free of tip and sample artifacts. All images presented here have been flattened by software routines.

A range of solution concentrations for which ordered adsorption could be achieved and observed with STM was determined. Solutions with a concentration of 8×10^{-7} M to about 3×10^{-4} M produced monolayers or multilayers of molecules easily imaged by STM. Less concentrated solutions did not form a monolayer, and hence no molecular order was seen. When solutions more concentrated than about 3×10^{-4} M were used, several layers of ordered molecules form on the surface, but their structure was obscured by the further adsorption of squaraine layers. Amorphous layers are composed of randomly adsorbed squaraine molecules without an ordered packing structure. The application of a short voltage pulse often removed these adsorbed molecules and briefly revealed the ordered squaraine layers. An image produced by this amorphous adsorption can be distinguished from the effects that are produced using a contaminated tip, since individual molecules within amorphous layers could often be resolved; however, their orientation within the layer was completely random. Hence, tip contamination is not an alternative explanation for the observance of this phenomenon. Often even when solutions within the range of acceptable concentrations (usually 10^{-5} to 10^{-4} M) were used, some amorphous adsorption did occur on top of the ordered multilayers. This small amount of adsorption could be enough to somewhat obscure the order of the layers beneath. When this occurred, a voltage pulse was applied to the surface, revealing the ordered layers.

Results and Discussion

Squaraines were found to be highly surface active molecules even when compared with other well-known 2D molecular systems. In one experiment 2-18 squaraine was dissolved into 4'-*n*-octyl-4-cyanobiphenyl (8CB) at a ratio of 0.1-5.0% wt/wt SQ/CB and deposited onto graphite. Although 8CB molecules were present in great excess, an ordered monolayer consisting solely of squaraine molecules was formed with no evidence of ordered 8CB molecules on the surface. Pure solutions of squaraine (with

concentrations within the range described above) formed ordered layers of squaraine that could be observed with STM shortly after deposition. The length of time elapsed between deposition and observation of adsorbed layers with STM ranged from several seconds to tens of minutes, depending on the identity of the squaraine. This time dependence will be explained in following sections. With the exception of 1-1 SQ and 2-18 SQ, the surfaces tended to show either no coverage or complete coverage, representing a step in the adsorption isotherm that is consistent with strong molecule-molecule interactions.

Squaraine molecules appear in most of our STM images as football-shaped areas of bright contrast measuring 15.0 ± 1.5 Å in length, 2.5 ± 1.5 Å in width, and from 0.7 to 1.5 Å in relative height. Images of particularly good resolution show two bright spots within the football-shaped region, each measuring ~ 3 Å in length (see image of 4-4 squaraine in Figure 4 and of 8-8 squaraine in Figure 6C). The length of the football shape corresponds well with the length of the chromophore of the molecule (from the nitrogen at one end of the chromophore to the nitrogen at the other end) with the spots assigned to the phenyl rings. The width of the football corresponds well with the width of a phenyl group, not including the oxygens and hydroxyls. The aromatic chromophore of the squaraine molecule should be imaged as an area of bright contrast, since this is where the majority of electron density is located in the molecule. In addition, this moiety is highly polarizable in contrast to the rather insulating alkyl tails. The oxygens not appearing as part of the bright contrast area, unlike the nitrogens, is explained by the theory proposed by Claypool et al. relating ionization potential to STM contrast.⁷ Essentially, atoms with high ionization potentials have a low probability for tunneling ($O \rightarrow$ dark contrast) whereas atoms with low ionization potentials have a high probability for tunneling ($N \rightarrow$ bright contrast). The lack of resolution of the alkyl tails of these squaraine molecules by STM is puzzling in light of the fact that *n*-alkanes and the tails of cyanobiphenyls have been routinely imaged on graphite surfaces.^{1-8,12,13,15-18} The length, width, and relative height of the bright football-shaped areas correspond well with a model of the molecule lying with the chromophore flat on the HOPG surface. Measured relative heights of 1-2 Å are typical for π systems adsorbed lying flat on the substrate surface, as measured by STM.⁴¹ Since the alkyl tails are not resolved, packing of the bright chromophores must be examined quantitatively to deduce the orientation of the tails.

Domain and Unit Cell Structure. Ordered layers of squaraines (with the exception of 4-4 SQ) were found to be highly stable and could be imaged continuously over periods of several days. These layers consisted of domains of tens of nanometers to several hundred nanometers in size. The domains within these layers were not stable, however, and tended to grow or contract over time, with smaller domains sometimes transforming into larger domains. This process of Ostwald ripening was observed most often and most obviously in samples of 1-1 SQ and 2-18 SQ. This can be seen in Figure 1, which shows a series of images of 2-18 SQ on HOPG which capture the process of domain nucleation and growth, and subsequent competition between domains. The shapes of domains exhibited by the squaraine series varied depending on the type of adsorbate structure that each squaraine produced. In general, squaraines that produced herringbone structures formed elliptical or rectangular domains and squaraines that produced row structures formed diamond-shaped, faceted domains. The differences in domain

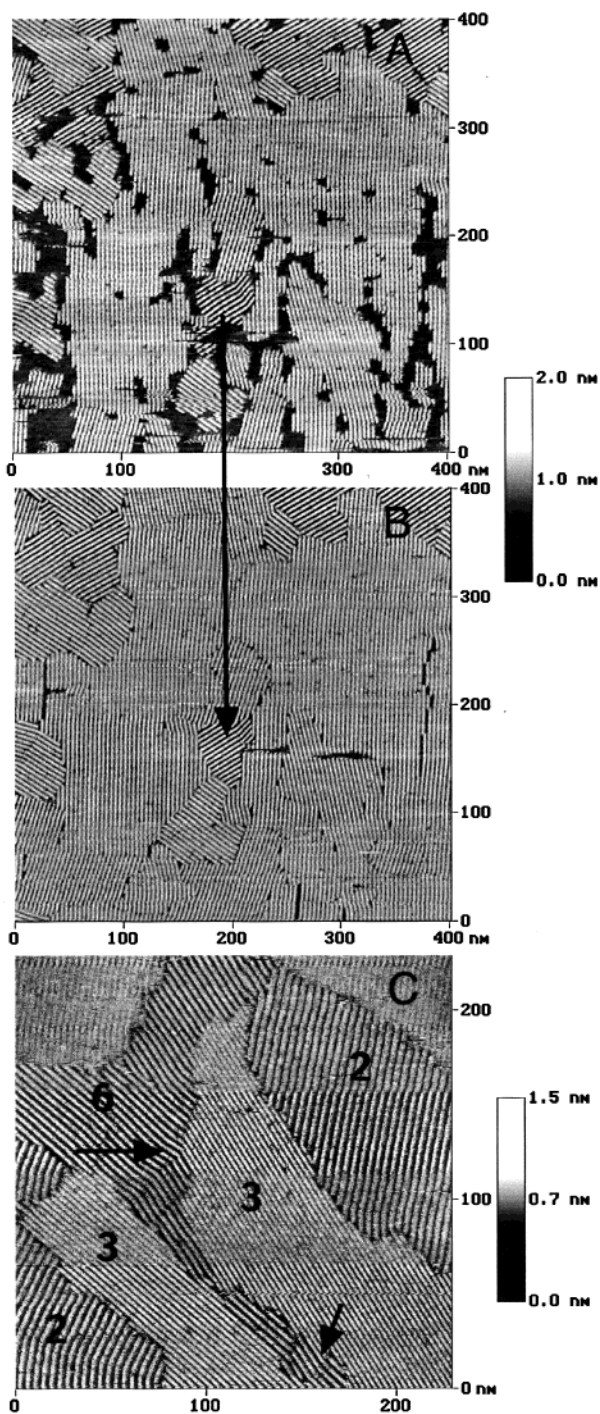


Figure 1. Three STM images of 2–18 squaraine adsorbed on HOPG. Images A and B are 400 nm \times 400 nm scans, taken 15 min apart, scan A being 5 min after deposition. Bare areas of HOPG can be seen in image A, whereas in image B the domains have grown substantially in size and almost fully cover the surface. In addition, one domain direction is becoming prominent. This direction does not correlate with the HOPG lattice. The arrow serves as a point of reference, indicating a domain cluster common to both images. Image C shows several domains of ordered 2–18 SQ molecules in which various widths of bright and dark rows are exhibited. Domain type 2 corresponds to polymorph no. 2 and exhibits 20 Å wide bright and dark rows, domain type 3 corresponds to polymorph no. 3 with 22 Å bright row widths and 15 Å dark row widths, and domain type 6 corresponds to polymorph no. 6 with 25 Å bright rows and 21 Å dark rows. Domain types 2 and 6 show a degree of flexibility in which rows are able to bend around each other. The arrows in image C point out smooth transformations from one structural phase to another.

stability, size, and shape will be elaborated upon in each of the individual squaraine sections.

1–1 Squaraine. Ordered regions of adsorbed 1–1 SQ were the most difficult of the five squaraine systems studied to observe with STM, with images of ordered 1–1 SQ layers being obtained only about 10% of the time. The lengths of the alkyl tail substituents have been shown to affect the conductivity of the molecular aggregates, with aggregates of the longer-tailed squaraines being the least conductive.⁴⁵ The higher conductivity of aggregates of 1–1 SQ may allow tunneling to occur more easily through its nonordered layers than tunneling for nonordered regions of longer-tailed squaraines. This may explain why 90% of the images obtained with STM of 1–1 SQ are of amorphous layers/regions. Thus, the amount of data acquired for 1–1 SQ is the smallest of those for the five squaraines studied.

When it is successfully imaged, as shown in Figure 2A, it can be seen that 1–1 SQ nucleates to form oblong, rounded domains of a few hundred nanometers in length which quickly grow together to cover the entire surface (Figure 2B) and frequently continue growing to form multiple layers. Isolated domains were extremely stable to the rastering motion of the tip but grew and shrank readily over time, presumably due to small temperature fluctuations. At scan sizes >100 nm, it was difficult to distinguish the molecular packing structure of 1–1 SQ, since individual molecules appear simply as an approximately 15 Å long and 2.5 Å wide football shape. When scan sizes were decreased to <100 nm, it was usually possible to resolve individual molecules within the ordered domains and determine the unit cell and subunit cell dimensions. The measured unit cell dimensions, calculated molecular areas, calculated packing densities, and other data for 1–1 SQ as well as all five squaraines are listed in Tables 2 and 3.

As seen in Figure 2C, 1–1 SQ exhibits at least three polymorphs. The first is a herringbone-like structure in which molecules intersect at 90° angles that we will refer to as the 90° herringbone (Figure 2C, region 1). The second and third polymorphs have been difficult to characterize unambiguously due to a lack of stable, small-scale, molecularly resolved images of these two polymorphs. However, they can be distinguished from one another in images. The unit cells for these latter two polymorphs have been determined through Fourier analysis and are listed in Table 2. The second polymorph appears to be a row/herringbone hybrid, in which adjacent molecules within the same row intersect with each other at $65^\circ/115^\circ \pm 5^\circ$ angles. We refer to this polymorph as herringbone-row (Figure 2C, region 2). The final polymorph appears to be a J-aggregate-like structure in which adjacent rows of molecules are staggered by half a molecular length with respect to one another (Figure 2C, region 3). We refer to this third polymorph as J-like. Of the three polymorphs, herringbone-row and 90° herringbone are observed most often and can coexist within the same domain and reversibly convert between the two forms, thus suggesting that they are of similar energy. The J-like-aggregate is very rarely seen, usually being converted into one of the other two polymorphs, and appears only in very small areas of a few hundred square nanometers. None of the polymorphs observed showed any registry with the surface.

As of yet, the only polymorph that has been imaged with high enough resolution to allow for unambiguous characterization is 90° herringbone. As a result, detailed discussion of the structures, intermolecular interactions, and polymorph conversions in the herringbone-row and J-like polymorphs will be deferred to a future paper. The

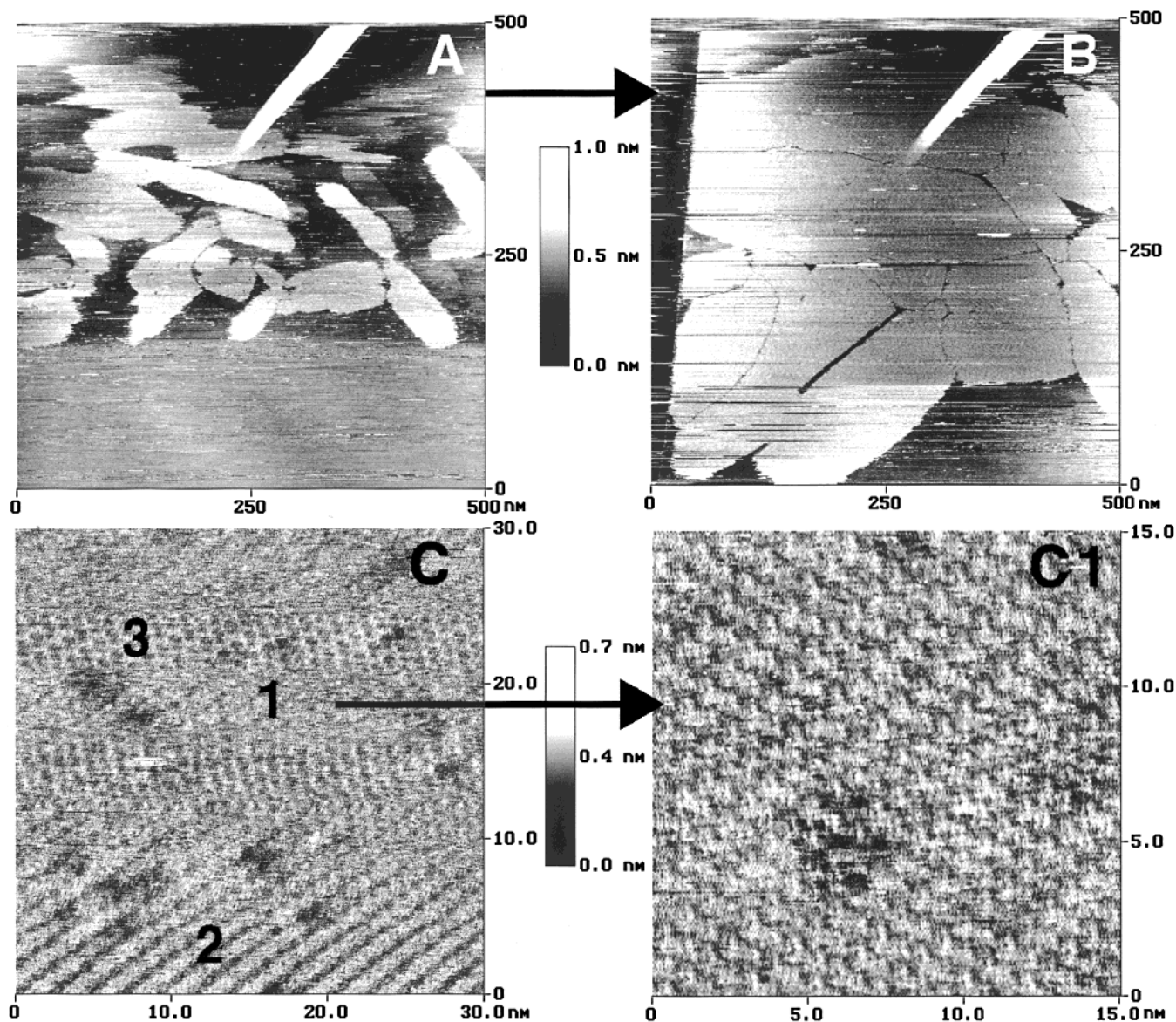


Figure 2. STM images of 1-1 squaraine adsorbed on HOPG. Images A and B show a time-lapsed sequence in which A was captured within 5 min of deposition and shows nucleation of oblong domains. B was captured 3 min after A and shows not only the growth of domains but also the relatively fast formation of multilayers. The numerous bright lines may be due to the presence of 1-1 SQ molecules trapped between the adsorbate layers and the tip which are dragged across the surface by the rastering motion of the tip. Image C shows a 30 nm \times 30 nm scan in which three different types of molecular packing coexist within the same domain. "90° herringbone", "herringbone-row", and "J-like" packing are shown in regions 1, 2, and 3, respectively. A zoomed-in image of "90° herringbone" is shown in C1. Lack of molecular resolution prevents showing similar zoomed-in images of the "herringbone-row" or "J-like" polymorphs.

90° herringbone polymorph will be the focus of the following discussion.

The close proximity of the molecules within the 90° herringbone phase (4.5 ± 1.5 Å between adjacent chromophores) presents a confusing case when trying to model the positions of the methyl tails of the 1-1 SQ molecules within the molecular packing. Unfortunately, the methyl groups are not resolved in any of the polymorphs, so their positions must be deduced from the orientation and distances between the observed molecular chromophores. The 90° orientation of the chromophores and the measured chromophore-to-chromophore distance of only 4.5 Å suggest that the dimethylamino moiety is rotated from the plane of the molecule, despite the loss of conjugation in the p system of the chromophore that this rotation would cause. If the methyls were in the same plane as the molecule, the distance between bright chromophores would be larger due to the steric repulsion between

adjacent molecules (at least 6.5 Å). In addition, methyls lying in the same plane as the chromophore might mitigate the interaction between positive and negatively polarized regions on adjacent molecules. It is this Coulomb interaction between negatively polarized oxygens and positively polarized nitrogens that appears to be the dominant molecule-molecule interaction between chromophores of adjacent 1-1 SQ molecules in the 90° herringbone polymorph. In addition, this structure appears to have donor-acceptor charge-transfer interactions. The donor moieties of each 90° herringbone squaraine molecule are pointed directly toward and are in close proximity to the acceptor moiety of two of the adjacent molecules (one on either side). Conversely, the acceptor moiety of each squaraine molecule is oriented with two donor moieties (1 from a molecule on either side) pointed toward and in close proximity to it. The 90° orientation of the squaraine molecules to one another may be the result of the

Table 2. Unit Cell Data for the Major Polymorphs of the Five Squaraines Studied^a

squaraine	packing structure	unit cell			packing density (molecules/nm ²)	molecular area (Å ² /molecule)
		α (deg)	a (± 1.5 Å)	b (± 1.5 Å)		
1–1	90° herringbone	90 \pm 2	25	25	0.64 \pm 0.08	156 \pm 19
	herringbone-row	100 \pm 1	15	8	1.53 \pm 0.24	66 \pm 10
	J-like	80 \pm 3	19	13	0.81 \pm 0.13	124 \pm 25
4–4	70° herringbone	85 \pm 3	19.5	18.5	0.55 \pm 0.10	180 \pm 30
	90° herringbone	90 \pm 2	29	29	0.48 \pm 0.05	210 \pm 23
8–8	row	72 \pm 5	27.5	8	0.45 \pm 0.14	220 \pm 56
12–12	type 1 row	84 \pm 5	28	7.5	0.45 \pm 0.13	224 \pm 56
	type 2 row	100 \pm 5	30	11.5	0.58 \pm 0.12	173 \pm 32
2–18	type 1 row		*		*	*
	type 2 row	90 \pm 2	42 \pm 2	8	*	*
	type 3 row		*		*	*
	type 4 row		*		*	*
	type 5 row		*		*	*
	type 6 row		*		*	*
	type 7 row		*		*	*

^a Asterisks represent a lack of data due to insufficient molecular STM resolution.

Table 3. Adsorption and Ordering Data of the Five Squaraines Studied

squaraine	ordered structure	observed bright row width (Å) (90° to row direction)	observed dark row width (Å) (90° to row direction)	expected bright row width (Å) (width of chromophore (N to N))	expected dark row width (Å) (length of alkyl tail)	angle of molecule to row (deg)	multilayers observed
1–1	90° herringbone	9 \pm 1	6.5 \pm 0.5	15	1	NA	yes
	herringbone-row					56/124 \pm 3	
	slipped-J					90	
4–4	herringbone	NA	NA	15	4–4.5	NA	no
8–8	row	14 \pm 1.5	11 \pm 1.5	15	9.5–10	68/112 \pm 3	yes
12–12	type 1 row	14 \pm 2	13 \pm 2	15	14–14.5	60/120 \pm 5	yes
	type 2 row	18 \pm 2	11 \pm 2				
2–18	type 1 row	18 \pm 1	21 \pm 1				
	type 2 row	22 \pm 2	20 \pm 2	15	1.5–2.2 (C ₂)	60/120 \pm 5	yes
	type 3 row	23 \pm 1	16 \pm 1		21–22 (C ₁₈)		
	type 4 row	23 \pm 1	24 \pm 0.5				
	type 5 row	26 \pm 1	16 \pm 0.5				
	type 6 row	26 \pm 1	21 \pm 0.5				
	type 7 row	30 \pm 2	14 \pm 2				

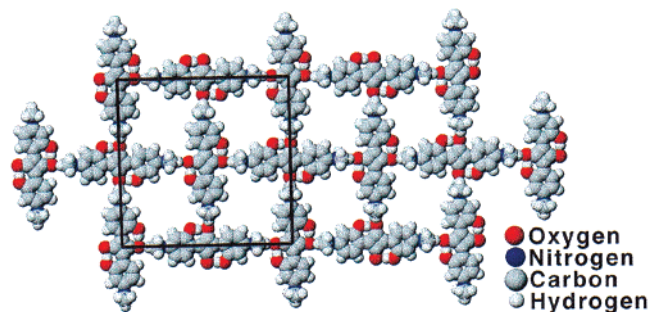


Figure 3. Molecular model proposed for the most stable of the three polymorphs exhibited by 1–1 squaraine when adsorbed onto the HOPG surface; “90° herringbone”. This was the only polymorph of 1–1 SQ for which high enough resolution STM images were obtained to be able to construct a packing model. The unit cell is represented by a black box.

dimethylamino groups being oriented almost perpendicularly to the plane of the molecule. As a result, all four of the molecules surrounding a single central molecule may orient at right angles to it at close enough proximity (4.5 \pm 1.5 Å) to allow donor–acceptor CT interactions to occur. A molecular model showing the orientation of 1–1 SQ molecules within the 90° herringbone polymorph is shown in Figure 3. The large surface area that is unoccupied within the 90° herringbone unit cell by squaraine molecules would appear to go against the trend of closest packing of 2D molecular adsorbates. We speculate that there are unimaged water molecules in these spaces that may stabilize the relatively open 90° herringbone unit cell structure through water–hydroxyl hydrogen bonding.

Other than this speculative hydrogen bonding, donor–acceptor and Coulomb forces appear to be the major molecule–molecule interactions directing packing in the 90° herringbone polymorph of 1–1 SQ and, in combination, may compensate for the proposed sterically induced loss in π conjugation that is caused by amino rotation out of plane. Additional work on the 1–1 SQ system is in progress at this time and will be published later.

4–4 Squaraine. Molecularly resolved 4–4 SQ adsorbate images were only slightly less difficult to acquire than those for 1–1 SQ. Images showing ordered domains of 4–4 SQ obtained within the first 0.5 h of squaraine solution deposition were of poor quality. The adsorbed domains were easily stripped off of the graphite surface, and the images were very noisy. Amidst the noise, small patches of clearly resolved molecules were observed (~ 10 nm \times 10 nm) in which a herringbone pattern of molecules consisting of bright football-shapes oriented at 90° \pm 2° to one another could be distinguished. Upon Fourier filtering of these patches, the 90° angle was confirmed. It is doubtful that these clearly-resolved patches of molecules were simply domain nuclei that then grew and stabilized. Micron-sized islands composed of a number of smaller domains of ordered molecules with only very slight variations in orientation with respect to other domains were usually evident a few minutes after solution deposition. Zooming in on small areas of the surface to achieve molecular resolution usually resulted in noise that then obscured most of the molecules within the domain except for the aforementioned few clear patches. Furthermore, this small area of clarity within a noisy domain did not

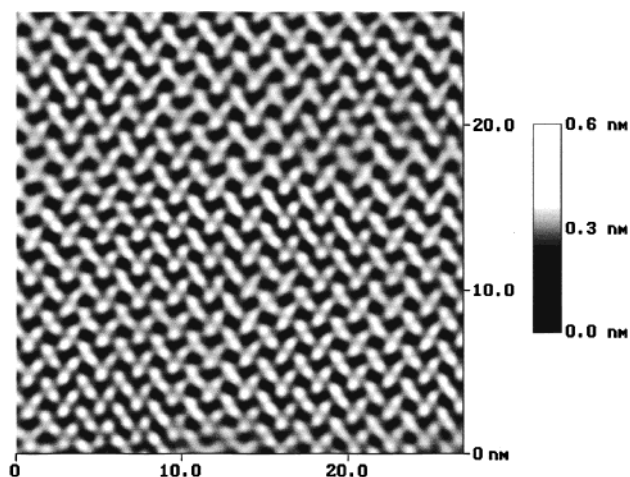


Figure 4. STM image ($27\text{ nm} \times 27\text{ nm}$) of the 70° angle herringbone phase of 4-4 squaraine adsorbed on the HOPG surface. The 90° and 80° angle phase structures were too transient to obtain high-quality images. In this image individual phenyl rings are visible within many of the bright squaraine chromophore “footballs”.

stay in one place. The noise became greater or lesser in different areas of the domain over time and thus exposed or obscured various parts of the domain at various times. Due to the excessive noise and poor quality of these images, they will not be presented in this paper. However, within minutes of the observance of the 90° herringbone phase, the adsorbate domains became clearer. Larger areas of the domains ($\sim 100\text{ nm} \times 100\text{ nm}$) now showed molecular resolution, were less susceptible to desorption, and were less noisy. Analysis of these more stable images showed that the angle between adjacent molecules within the herringbone pattern changed to $70^\circ/110^\circ \pm 3^\circ$ (as seen in Figure 4). All further images of 4-4 SQ domains showed a $70^\circ/110^\circ$ angle between adjacent molecules until the system became unable to be imaged ($\sim 5\text{ h}$). This behavior was reproducible from session to session.

Despite this reproducible increase in image clarity, only about one session in 10 resolved the individual phenyl rings within each football shape. One imaging session revealed a patch of molecules during the transition from 90° to 70° which exhibited an $80^\circ/100^\circ$ angle. Due to excessive noise in the images, the few images of this 80° phase are not shown here. Lack of clarity in the images also prevented us from obtaining unit cell measurements for this 80° phase. Unit cell measurements for the 90° and 70° herringbone phases, however, are listed in Table 2. A metastable 80° phase may be an intermediate phase in the 90° to 70° transition.

The three polymorphs observed for 4-4 SQ differ only in the angles between adjacent molecules. The 80° and 90° structures appeared only briefly at the onset of ordering, with 90° converting into 80° and 80° into 70° . The 70° polymorph was observed to be the most stable structure. In order for D-A or Coulomb interactions to occur, the nitrogen must be oriented close to the acceptor moiety. This necessitates that the nitrogen be “exposed” to an adjacent molecule. Thus, the alkyl tails can either lie on the graphite surface perpendicular to the long axis of the molecule, as modeled in Figure 5A, or protrude from the surface into the solvent, as modeled in Figure 5B. If the tails are oriented perpendicular to the molecule and on the graphite surface, then the optimum packing appears to be when the adsorbed molecules are oriented at 90° to one another. This minimizes the distance between nitrogen donor and acceptor, producing a stronger inter-

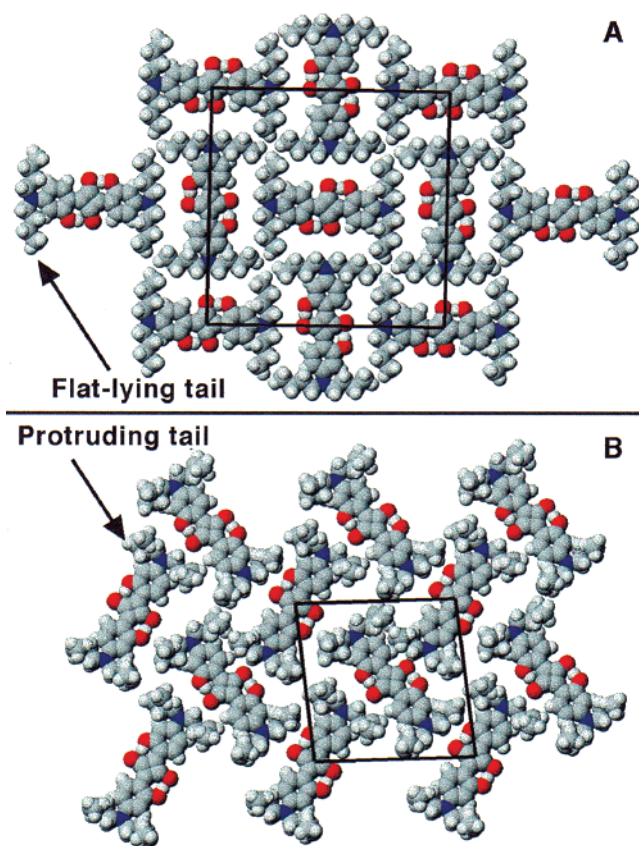


Figure 5. Molecular models of two of the three polymorphs exhibited by 4-4 squaraine on HOPG. Model A shows the structure proposed for the initial 4-4 polymorph with 90° herringbone packing. All four butyl tails of the adsorbed 4-4 molecules must lie perpendicular to the long axis of the molecule if they are to lie on the HOPG surface. Model B shows the structure proposed for the final polymorph which exhibits a 70° herringbone packing. The butyl tails may still lie perpendicular to the long axis of the molecule; however, they must partially desorb (some of the methylene units must protrude up from the surface) in order to adopt the $70^\circ/110^\circ$ angle of orientation to one another. The third polymorph (not shown) is an intermediate between the 70° and 90° structures in which an $80^\circ/100^\circ$ configuration is taken. This polymorph is too unstable for accurate unit cell determination; as a result, no model is proposed.

action. However, this 90° packing quickly transforms into an intermediate 80° structure that is too unstable for accurate unit cell measurements.

Our modeling shows that the rotation of molecules from 90° to each other to the 70° packing structure requires the alkyl tails to desorb from the surface and protrude up into the solvent. Their process is sterically hindered if the tails remain on the surface while the molecules rotate from 90° to 70° . The intermediate 80° phase may have only alkyl tails from one side of the molecule protruding into the solvent. Neither the 70° nor the 90° structures show any alignment with the major surface lattice vectors, so commensuration is not an explanation for the stability of one phase with respect to another (refer to Orientation with Respect to HOPG section). One explanation is that the 70° phase is more entropically favored due to more degrees of freedom from the freely rotating protruding alkyl tails. There may also be a slightly larger packing density for the 70° phase, but the quantitative estimates are within the experimental error for both phases (Table 2).

8-8 Squaraine. Unlike 1-1 SQ and 4-4 SQ, 8-8 SQ was found to form stable domains of adsorbed molecules

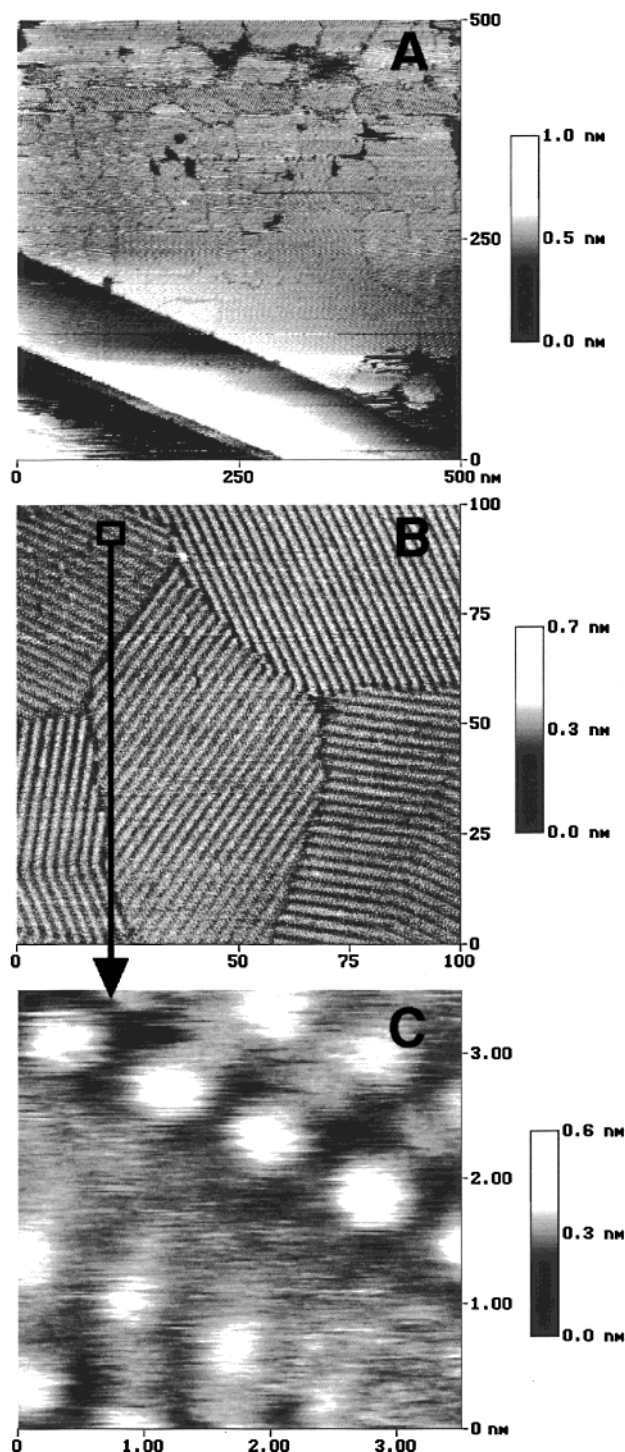


Figure 6. Three STM images showing the ordered adsorption of 8-8 squaraine on HOPG. Image A is a 500 nm \times 500 nm scan showing multiple layers of molecules ordered in numerous and relatively small domains of molecular rows. Image B shows five domains of different orientations of 8-8 rows in a 100 nm \times 100 nm area. A zoomed-in portion of the top left domain is shown in C. Individual molecules within the rows are clearly seen as a pair of spots, the spots being the phenyl rings.

that produced clear STM images. Almost immediately upon deposition of the 8-8 SQ solution onto the HOPG surface, monolayer and sometimes multilayer coverage of ordered domains was observed in the STM images (see Figure 6A). Unlike the 1-1 SQ and 4-4 SQ domains, which were of elliptical or square-like shape, domains of 8-8 SQ were diamond-like in shape with angular edges, or facets. They were typically about 100 nm in length and

about 50 nm in width and were composed of alternating bright and dark stripes, as can be seen in Figure 6B. Domains of ordered 8-8 SQ molecules were extremely stable and could be imaged continuously over the course of several days without much change in structure, except for the formation of multiple layers.

At small scan sizes, molecular and submolecular features of 8-8 SQ adsorbate structures could be resolved. The bright stripes, measuring $15 \text{ \AA} \pm 1.5 \text{ \AA}$ in total width, consisted of a column of bright football shapes stacked in a row. This width is consistent with the length of the squaraine chromophore (from the nitrogen at one end of the molecule to the nitrogen at the other end: 15 \AA). About 50% of the time a pair of bright spots within each football shape could be resolved, an example of which is shown in Figure 6C. These spots were assigned to the phenyl rings in the squaraine chromophore. No features could be distinguished within the dark stripes, however, which typically measured $11.0 \pm 1.5 \text{ \AA}$ in width. This distance corresponds well with the length of an octyl tail ($\sim 10 \text{ \AA}$). The heights measured by STM for the bright stripes relative to the dark stripes (0.8 to 1.5 \AA) are relative heights typical for π systems adsorbed lying flat on the HOPG surface,⁴¹ suggesting that the chromophore of the molecule is likewise lying flat on the HOPG surface. The distance between pairs of bright spots within the same stripe was measured to be $4 \pm 1 \text{ \AA}$. This relatively close spacing between adjacent squaraine chromophores within the same row requires that only one of the octyl tails of each dialkylamino group can lie flat on the HOPG surface. If both tails lie on the surface, a minimum distance of 12 \AA between adjacent chromophores within the same row would be needed so that alkyl tails from adjacent molecules would not sterically interfere with each other. This row structure, in which the chromophores of the molecules are widely spaced, is not observed and furthermore would be very unfavorable, since there is a well-known strong interaction between adjacent chromophores that is not present in this structure. Instead, one tail from each dialkylamino might protrude up from the surface and be solvated by the phenyloctane solvent or it may form a second ordered alkyl layer. Evidence of this kind of three-dimensional adsorbate structure has been reported by Gorman et al. in their study of the ordered adsorption of the didecylamino molecule DAPDA.⁵⁹ Recognizing the similarity in structure between the DAPDA and the alkyl portions of the squaraine molecules, it is tempting to assign the same molecular conformation to the second tail in both 8-8 SQ and DAPDA, since the nonplanar functional group is the same for both molecules except for the length of the alkyl tails. For squaraines, however, it appears that protruding alkyl groups are only possible in monolayers or in the case of the topmost ordered layer. When multilayers of squaraine molecules are imaged, the relative height of the edge of each layer is $2.5 \pm 0.5 \text{ \AA}$. Although STM does not measure actual heights, the small magnitude of this distance (still very close to the typical $1\text{--}2 \text{ \AA}$ relative height measured via STM for planar aromatic molecules lying flat on the HOPG surface) makes it very doubtful that alkyl tails of molecules that are not in the topmost molecular layer should be protruding perpendicularly. In sandwiched layers the remaining two alkyl tails must lie either on top of the planar tail or on top of the chromophore. Remaining alkyl tails lying coplanar with the molecular plane (lying on the HOPG surface if in the first molecular layer) most likely inter-

(59) Gorman, C. B.; Touzov, I.; Miller, R. *Langmuir* **1998**, *14*, 3052-3061.

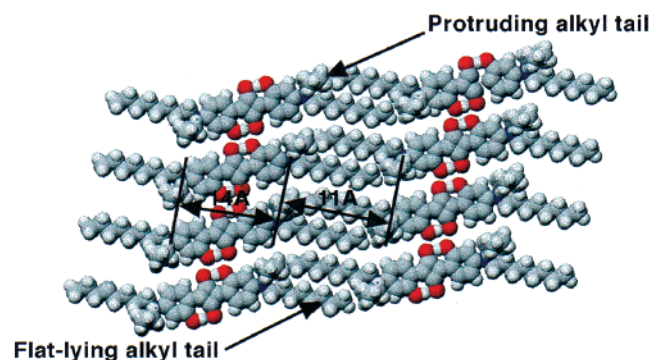


Figure 7. Molecular model showing the proposed row-packing structure of a monolayer or topmost adsorbed layer of 8-8 squaraine on HOPG. One tail from each dialkylamino group lies coplanar with the chromophore on the HOPG surface while the other tail protrudes up from the surface into the phenyl-octane solvent. Molecular layers of 8-8 which are sandwiched between a bottom and topmost layer most likely do not have this structure, since the protruding tails would be sterically hindered by the presence of the layer above. Instead these tails may lie atop either the coplanar tails or the chromophore.

digitate, such that tails from molecules in adjacent rows lie side by side. Thus, in addition to the molecule-substrate interactions between adsorbed alkyl tails and the HOPG lattice, a new intermolecular interaction is introduced by the formation of rows of molecules: dispersion forces between interdigitated alkyl tails.

By measuring the angle between the direction of the bright stripe and the long axis of the bright football shapes within the stripe, it was found that the 8-8 SQ molecules within a row are found to orient $68/112 \pm 3^\circ$ to the direction of the row. This angle results in an offset between adjacent molecules of $\sim 2.5 \pm 0.5$ Å, allowing alignment of their respective donor and acceptor moieties. The proposed model of this molecular packing is shown in Figure 7. This structure is very similar to the "slipped-stack variant structure" proposed by Law et al. for 1-1 SQ (nonhydroxylated) solution aggregates.⁶⁰ Hence, the D-A interaction between adsorbate molecules is preserved in the row structure despite the introduction of dispersion interactions of alkyl tails with other alkyl tails and the substrate. A third intermolecular interaction is possible between molecules in a row that are offset by 2.5 Å. This offset combined with the 4 Å distance between adjacent phenyls puts one of the oxygens of the square core within 2 Å of a hydroxyl hydrogen of the neighboring squaraine within the same row. Hence, hydrogen bonding may be possible between adjacent squaraines. Whether it is a driving force for the formation of the row structure is uncertain. Studies are currently under way in our laboratory to determine the influence of hydrogen bonding on the structures formed using the corresponding nonhydroxylated squaraines.

12-12 Squaraine. Like 8-8 SQ, 12-12 SQ molecules adsorb in row structures and order in layers of oriented domains within minutes of solution deposition onto the graphite surface, as can be seen in Figure 8A. Unlike the case of 8-8 SQ, two different types of 12-12 SQ domains were observed defined by their differing stripe widths. Bright stripes in the first domain type were measured to be 14.0 ± 2 Å in width, and dark stripes were 13 ± 2 Å wide, whereas in the second domain type bright stripes were measured to be 18 ± 2 Å wide and dark ones were 11 ± 2 Å wide. In addition, the second type appeared to be composed of two football shapes across its width (see

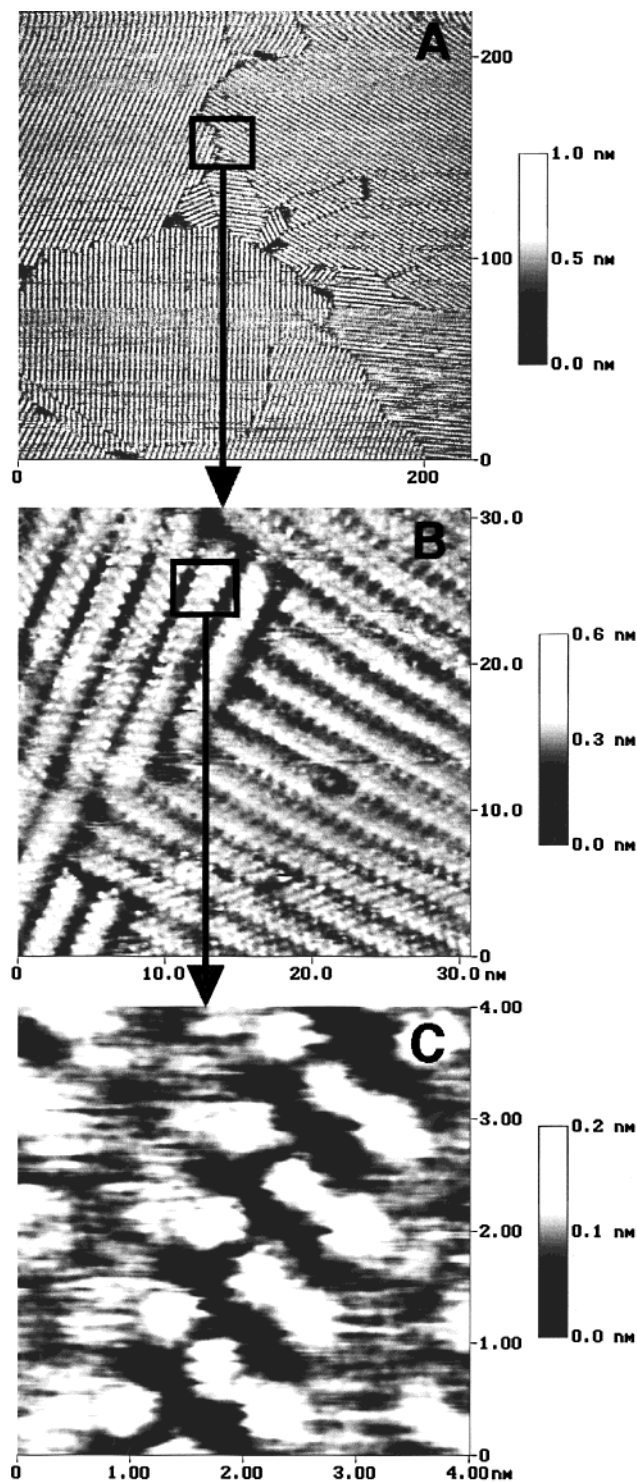


Figure 8. Three STM images showing the ordered adsorption of 12-12 squaraine on HOPG. Each image is a zoomed-in portion of the image above it. Image B is a $32 \text{ nm} \times 32 \text{ nm}$ scan that appears to show bimolecular rows, the width of each row consisting of two to three bright spots which altogether measure 18 ± 2 Å in width. Image C is a $4 \text{ nm} \times 4 \text{ nm}$ scan that shows one of the rows of three bright spots. We propose that the three-spot rows measuring ~ 18 Å in width are due to the adsorption of a second layer of molecules commensurate but offset from the first such that the two layers are not distinguished with STM. Figure 11B shows a model of this bilayer structure.

Figure 8B), which when zoomed in upon at scan sizes of $\sim 10 \text{ nm} \times 10 \text{ nm}$ often revealed a set of 3 or 4 spots (see Figure 8C). Again, no features could be distinguished within the dark stripes for either polymorph. With the exception of the widths of the bright and dark stripes and

(60) Law, K. Y. *J. Phys. Chem.* **1988**, *92*, 4226-4231.

the unit cells, all other parameters measured for the two polymorphs were the same (see Table 3). The angle of the long axis of the football shapes to the direction of the row was measured to be $60/120 \pm 5^\circ$, while the distance between football shapes within the same row along the length of the row was $4 \pm 1 \text{ \AA}$ for both polymorphs. The height of bright stripes relative to dark was measured to be in the range of 0.8 to 2 \AA . In addition, both polymorphs exhibited domains of similar sizes and shapes, ranging from small, diamond-like shapes of tens of nanometers in length and width to larger, less well-defined shapes of $\sim 100 \text{ nm}$ in length and width. Layers of 12–12 SQ containing both polymorphs of domains were found to be stable, generally free of noise, and capable of being imaged continuously over the course of several days.

The widths of the stripes in polymorph type 1 are easily explained on the basis of the model of the row structure adopted by 8–8 SQ when adsorbed on the graphite surface. The bright rows of $14 \pm 2 \text{ \AA}$ width and dark rows of $13 \pm 2 \text{ \AA}$ are consistent with the length of the squaraine chromophore at a 60° angle to the row ($\sim 12 \text{ \AA}$) and with the length of the dodecyl tail ($\sim 14 \text{ \AA}$). These measurements, as well as that of the 0.8 – 2 \AA relative height, suggest that, like 8–8 SQ, molecules of 12–12 SQ in the type 1 phase adopt a conformation on the surface in which the chromophore of the molecule and one dodecyl tail from each dialkylamino moiety lie flat on the HOPG surface. The 60° angle between the long axis of the chromophore and the direction of the row results in an offset between adjacent molecules within the same row such that donor and acceptor moieties of adjacent molecules are aligned. This is analogous to the structure proposed for 8–8 SQ in which molecules align flat on the graphite surface in a J-like aggregate formation with one tail from each dialkylamino group lying on the graphite interdigitated with the tails from the adjacent row. Despite the addition of 16 methylene units in the transition from 8–8 SQ to 12–12, the adsorbate structure observed is essentially the same for both and donor–acceptor interactions still appear to play a significant role. Figure 9A shows the proposed molecular model for 12–12 SQ single-layer packing.

Polymorph 2 of 12–12 SQ does not follow this model. For this molecule the width of bright stripes ($18 \pm 2 \text{ \AA}$) is longer than the chromophore length from nitrogen to nitrogen (15 \AA). Since the alkyl tails do not contribute significantly to the tunneling current measured by STM for adsorbed squaraines, we find it plausible to attribute this increase in bright row width to multilayer imaging in which rows of molecules from two adjacent molecular layers are slightly offset from one another ($\sim 4 \text{ \AA}$) but are not resolved by STM. We call these proposed structures bimolecular rows. A small number of STM images were obtained which show a gradation in contrast across the width of the bright rows. The brightest portion of the width was measured to be $\sim 14 \text{ \AA}$ wide and $\sim 0.8 \text{ \AA}$ in relative height, as compared to the rest of the bright row, which measured 4 \AA in width and $\sim 0.5 \text{ \AA}$ in relative height. These measurements provide evidence for a multiple-layer structure. These images, however, will not be presented here. Figure 9B shows a structure incorporating two molecular layers, both of Figure 9A type packing. In this structure molecules in the second layer are parallel to, but offset from, molecules in the first layer such that two separate interlayer D–A interactions are possible between each pair of molecules (one originating from the first layer and one from the second). A pair is now defined as a molecule in the first layer and the molecule in the second layer directly above it. The second-layer molecule overlaps

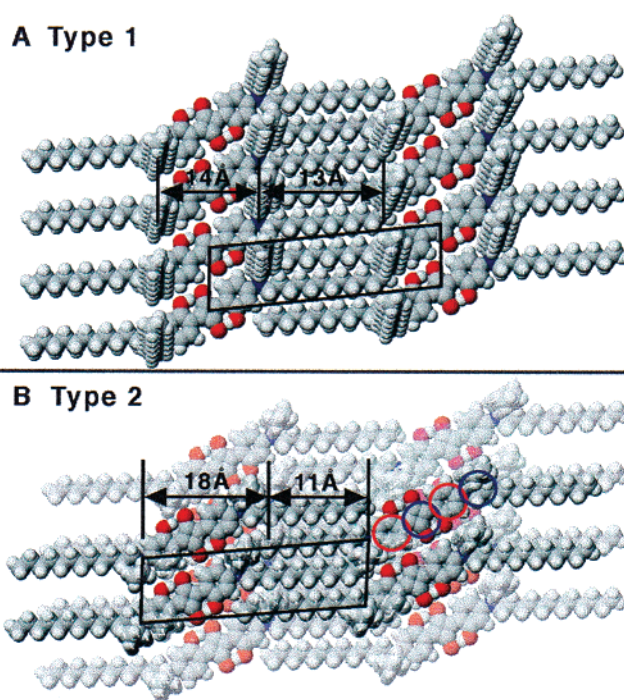


Figure 9. Molecular models of the proposed packing of 12–12 squaraine on HOPG corresponding to the two types of rows observed. Model A shows two adjacent molecular rows within the same molecular layer. This structure corresponds to a bright row width of 14 \AA and a dark row width of 13 \AA (type 1). Model B shows a second molecular layer (highlighted) adsorbed on the first (shadowed) which corresponds to a bright row width of 18 \AA and a dark row width of 11 \AA . The molecules in the second layer are commensurate with but offset from the positions of the molecules in the first such that the donors and acceptors within the two layers may align. If the STM tip does not distinguish between molecules in the two layers, then the bright rows may appear wider than a type 1 bright row and the dark rows narrower. This is assuming that the chromophores alone (regardless of proximity to the tip) contribute to bright contrast and a lack of chromophore produces a dark region. The circles indicate positions of phenyl groups in both layers that may be contributing to the increased tunneling current of a bright row. Red circles correspond to the position of a phenyl group in the second (top) layer, and purple ones to phenyl groups in the first (bottom) layer.

with the molecule below such that its acceptor group and one of its donor groups overlap with one of the donors and the acceptor group of the molecule in the layer beneath. Due to the 4 \AA offset, a 4 \AA portion of the alkyl tail (or dark row) of the first layer is eclipsed by the bright chromophore of the second-layer molecule. This may explain the reduction in the width of the dark rows to $11 \pm 2 \text{ \AA}$ and the increase in width of the bright rows to $18 \pm 2 \text{ \AA}$, both within experimental error of the expected widths of 16 \AA and 9 \AA , respectively.

2–18 Squaraine. 2–18 SQ is the only squaraine represented within the series presented here that has different alkyl tail lengths within the same molecule. In addition, it has the longest alkyl tail of any squaraine within the series, its stearyl tails being 6 methylene units longer than a dodecyl tail, yet its ethyl tails are only 1 methylene unit longer than the shortest tail in the series (methyl). This difference resulted in some special characteristics of the adsorption and ordering of 2–18 SQ onto the HOPG surface when compared to the other squaraines. Upon deposition of a 2–18 SQ/phenyloctane solution onto the graphite surface, ordered domains of 2–18 SQ were imaged almost immediately, however, almost always as isolated domains which then grew together over time and

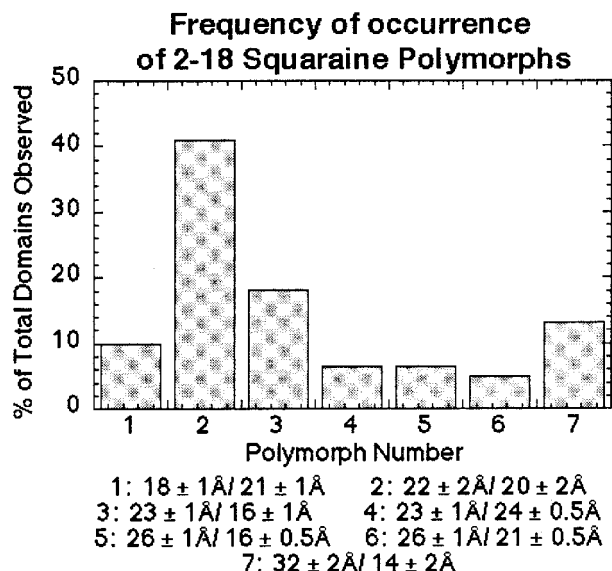


Figure 10. Histogram showing the frequency of observation of the seven different polymorphs of the 2-18 SQ ordered adsorbate structure. Polymorphs 2 and 3 are the two most frequently observed structures. Figure 11 shows a model of a proposed structure for polymorph 2.

eventually formed multiple layers (see Figure 1A and B). The only other squaraine that was observed at submono-layer coverages was 1-1 SQ, although, unlike 1-1 SQ, adsorbed domains of 2-18 SQ were free of noise and easily imaged. Although domains of ordered 2-18 SQ consisted of alternating bright and dark stripes (as in 8-8 SQ and 12-12 SQ), rather than being diamond-like and angular (as in 8-8 SQ and 12-12 SQ), domains of 2-18 SQ instead were meandering and irregularly shaped compared to those of 12-12 SQ and 8-8 SQ. Bright stripes of adsorbed 2-18 SQ were often found to bend around corners and merge with other bright stripes (see Figure 1C). In addition, upon inspection of hundreds of 2-18 SQ domains, it was discovered that 2-18 SQ produces a wide variety of bright and dark stripe widths, as listed in Table 3 and shown by their frequencies of observation in Figure 10. All the rows showed a 60° angle between the molecules within the row and the direction of the row. All bright stripes were measured to have vertical heights of 1-2 Å relative to the dark stripes.

The lower symmetry of the 2-18 molecule allows for a different structural conformation than that of the other long-tailed squaraines that form row structures. The small size of the ethyl tails, on either side of the 2-18 squaraine molecule, allows for the ethyls to lie coplanar with the chromophore and the stearyl tails. This is not possible for the more symmetrical long-double-tailed squaraines because, as described in the section on 8-8 SQ, the coplanarity of the tails would preclude the formation of the observed close-packed structure. This structure, in which all four of the alkyl tails lie flat within the same plane, alters the degree of interdigitation that is possible between the stearyl tails of molecules in adjacent rows. Because the ethyl tails are occupying space within the plane of the stearyl tails, stearyls from molecules in the adjacent row cannot interdigitate to the degree that is seen in 8-8 SQ and 12-12 SQ row structures. As a result the width of the portion of the alkyl tail rows appears larger than the actual length of the tails (see observed dark row width and expected dark row width measurements for 2-18 SQ in Table 3). The dark row widths of 8-8 SQ and 12-12 SQ, however, were roughly equal to the lengths of the octyl and dodecyl tails, respectively. A

model representing a single-layer row structure for 2-18 SQ was produced on the basis of (1) the measured angle of the long axis of the squaraine chromophore to the direction of their molecular rows, (2) the measured distance between adjacent molecules within the same row, (3) the length of the chromophore, and (4) the assumption that all four alkyl tails are interdigitated and coplanar on the HOPG surface. This particular model structure would produce a bright row width of approximately 12 Å and a dark row width of approximately 29 Å. A model of this single-layer packing is shown in the top (highlighted) layer of Figure 11B. However, a polymorph fitting these measurements was not observed. In fact, none of the polymorphs observed exhibited bright row widths of <17 Å. Again, like the case for 12-12 SQ, the observation of bright row widths >12 Å suggests that additional molecular layers are formed but are not molecularly resolved by STM. Since all seven of the 2-18 SQ polymorphs observed exhibited bright row widths of >12 Å, we assume that they are all composed of multiple layers of 2-18 molecules with various orientations of adjacent layers. It is not clear why a single-layer 2-18 SQ structure was never observed. Solutions of relatively dilute concentration were used to try to prevent multiple-layer adsorption, but with no success. Either multiple-layer adsorption was observed or no adsorption was observed. The coplanarity of the ethyl tails with the chromophore and the stearyl tails may allow 2-18 chromophores in adjacent layers to come closer to one another, making interlayer D-A interactions and thus multilayering more favorable than that with more symmetrical long-tailed squaraines. For example, one dodecyl tail from each side of 12-12 SQ must lie between molecular layers, since it cannot adopt a coplanar conformation. The presence of these tails may prevent molecules from getting as close to one another as is optimum for multilayering. Thus, it may be that the lower symmetry of the 2-18 molecule promotes multilayering more so than that of the symmetrical squaraines.

Due to the large number of polymorphs exhibited by 2-18 and the difficulty in resolving individual molecules within molecular rows (making unambiguous assignment of structure difficult), only the major polymorph of 2-18 SQ will be discussed in detail. The no. 2 polymorph is the most frequently observed 2-18 SQ polymorph and exhibits a bright row width of 22 ± 2 Å and a dark row width of 20 ± 2 Å. Figure 11 (A and B) shows a molecular model that may explain the measurements. Using the packing arrangement of the single-layer structure mentioned above (which was not observed by itself), three molecular layers of this packing are adsorbed atop one another such that the second layer is parallel to but offset from the first by 4 Å and the third is parallel but offset from the second by 4 Å. This trilayer structure is analogous to the type 2 structure proposed for 12-12 in which two donor-acceptor interactions are present between every pair of molecules; however, the addition of a third layer introduces a second pair to the structure. Pair 1 is the molecule from the second layer and the molecule in the first that it is overlapping, and pair 2 is the molecule in the third layer and the molecule in the second layer of the first pair that it is overlapping. Of course, dispersion interactions between tails lying atop one another in adjacent layers are also possible. The eclipsing of a total of 8 Å of the tail length by the chromophores of the second and third layers produces a dark row 21 Å in width instead of the 29 Å full width. The extension in length of the chromophore by 8-9 Å produces a bright row of 21 Å width instead of the 12 Å width of the single-layer structure. The observed bright and dark row widths are within experimental error

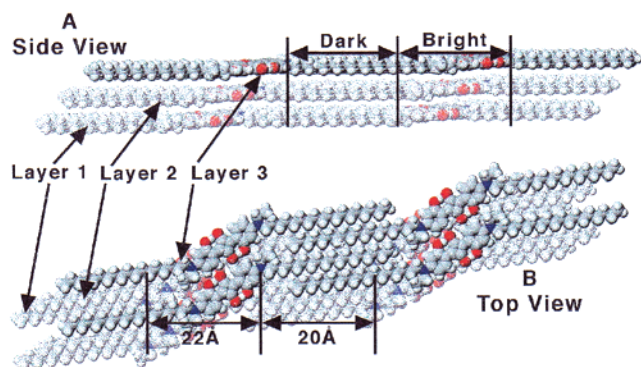


Figure 11. Molecular model representing a possible structure for the most commonly observed row structure polymorph of 2–18 SQ adsorbed on HOPG. This polymorph (no. 2 from Table 3) exhibits bright rows of 23 Å width and dark rows of 20 Å width. A possible structure corresponding to these measurements consists of three separate layers of 2–18 SQ ordered in rows in which each layer is commensurate with the layer below but is offset by approximately 4 Å, such that donor and acceptor moieties between the two layers may align. The bright rows correspond to the total width of the three layers of overlapping chromophores whereas the dark rows correspond to areas lacking in chromophore (areas of only alkyl tails). Other polymorphs exhibited by 2–18 SQ may be variations of this model in which multilayer structures are formed, but the distances between molecules in adjacent rows are either greater or lesser (alkyl tails are interdigitated to varying degrees) or the number of layers producing the polymorph is different, thus producing different bright and dark row widths, as observed by STM.

of the expected row widths for this molecular model (22 ± 2 Å for the bright row and 20 ± 2 Å for the dark row).

The remaining six observed polymorphs of 2–18 SQ also appear to be multilayer structures. Variation in degrees of overlap between chromophores of molecules in adjacent layers may be one of the factors producing the different observed row widths. This overlap variation may also allow different interlayer interactions to occur than the donor–acceptor interaction that appears to drive the no. 2 polymorph. For example, an offset of ~ 7.5 Å between adjacent layer chromophores allows a slightly different donor–acceptor interaction to occur in which the electron-donating amino group of one of the chromophores in the pair and the electron-accepting central ring of the second chromophore overlap one another. A dipole–dipole interaction may be introduced with an offset of ~ 12 Å, which allows the C–N bond linking the amino nitrogen and the phenyl of one molecule of a pair to overlap the same bond in the second molecule of the pair. The C–N bonds overlap each other such that the positively polarized N of one molecule overlaps the negatively polarized C of the other molecule and vice versa.

As mentioned in the very beginning of the Results and Discussion section, 2–18 SQ adsorbed from 8CB maintained the same packing structures and unit cell dimensions as 2–18 SQ adsorbed from phenyloctane. The major difference between the two systems is the number and size of squaraine domains and the occurrence of diamond- and triangle-shaped defects within squaraine rows (see Figure 12A). Both these effects can be understood when the large excess of 8CB in the binary system is considered. Although the beginnings of nucleation of squaraine domains from the 8CB melt were never directly observed with STM (the 2–18 SQ nucleation time scale from the 8CB melt being much faster than the time scale of imaging), it can be assumed that initially the surface is occupied by 8CB, due to its great excess. 2–18 SQ

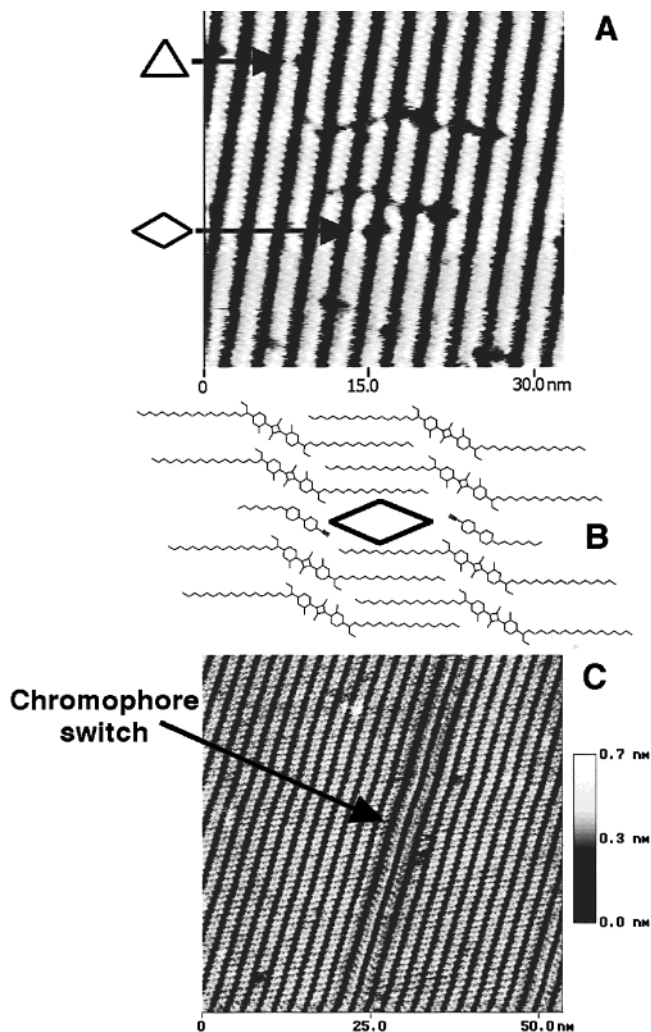


Figure 12. (A) STM image ($35 \text{ nm} \times 35 \text{ nm}$) showing a typical domain of ordered 2–18 squaraine adsorbed from a solution of 99% wt/wt 8CB. Numerous diamond and triangle defects can be seen within this domain. We propose that triangle defects are caused by single 8CB molecules trapped within the row structure of 2–18 SQ, whereas diamond defects are a pair of 8CB molecules trapped in adjacent squaraine rows. (B) Simple model showing how a pair of correlated triangle defects may form a diamond defect. A single-layer 2–18 SQ row structure is used for the sake of simplicity. (C) STM image ($54 \text{ nm} \times 54 \text{ nm}$) showing another type of defect commonly observed in images of 2–18 SQ adsorbed from an 8CB melt: the arrow points out two rows within a domain whose chromophores are oriented in the opposite direction to that of the chromophores in adjacent rows.

molecules must then adsorb into 8CB voids or displace 8CB molecules (most likely two at a time). Having reached a critical diameter, 2–18 SQ nuclei grow and spread across the HOPG surface, replacing the adsorbed 8CB. This competitive growth process may account for the numerous small domains arising from 2–18 SQ adsorption from 8CB. 8CB can become trapped within the 2–18 SQ monolayer, causing a disruption of the local squaraine packing, and thus a defect. A single 8CB molecule trapped within a row of squaraine molecules may be the cause of the triangle-shaped defects observed. A diamond-shaped defect may be the effect of two correlated triangle defects arising from the presence of two 8CB molecules trapped directly across from each other in adjacent rows, as is illustrated in Figure 12B. It has been observed that when a molecule is missing from an interdigitated row structure, the molecule across

from it is destabilized and often leaves the row as well.⁶¹ These two squaraine vacancies can be easily filled by 8CB molecules, resulting in a diamond-shaped defect.

Another type of defect that was observed regularly when 2–18 SQ was adsorbed from an 8CB melt can be seen in Figure 12C. An isolated row within a domain whose chromophores are aligned in the opposite direction to that of the chromophores in all the other rows within that domain can be seen in the figure. Such defects were also observed in layers adsorbed from squaraine/phenyloctane solution, however, less often than in those from squaraine/8CB melts. A molecular model for this opposite chromophore direction will not be proposed herein.

Multilayers. Multiple layers of squaraine adsorption and ordering were observed consistently for every squaraine system studied except 4–4 SQ, as can be seen in Table 3. Figure 13A shows an image obtained from a 8–8/12–12 (10/1) squaraine mixture where four layers of ordered molecules grown one on top of another can be seen. These multiple layers usually occurred when concentrations of squaraine in phenyloctane $> 1.0 \times 10^{-6}$ M were used. About 70% of the overlayer domains coincided with the domain direction of the molecules directly beneath them. The remaining overlayer domains, not in registry with the domain just beneath, tended to be oriented at a 60°/120° angle to the lower domain. Crisscrossing of rows in adjacent layers occurred, often forming a crosshatch pattern, as can be seen in Figure 13B. This figure also provides a method to distinguish between a squaraine layer that is adsorbed atop a graphite terrace and squaraine multiple layering. In our images squaraines that are adsorbed atop a graphite terrace always show a stripe of what we think are nonordered molecules along the edge of the graphite step, as can be clearly seen in Figure 13B. The relative height measured between the adsorbate and the terrace below is always within experimental error of the sum of the height of the molecular layer and a multiple of the interplane distance of graphite (~ 3.4 Å). As can be seen in Figure 13A, squaraine layers show an abrupt end to the stripes of the domains that lie at the step edge, with no border stripe. The relative height measured for the molecular terraces was always found to be 2.5 ± 0.5 Å or some multiple of this height.

Since the first work reporting the study of molecular adsorbate systems with STM,^{62–64} the generally accepted model of STM imaging assumed that only the first layer of adsorbed molecules on a conducting/semiconducting substrate is imaged by the probing tip. In fact there are often many layers of molecules with varying degrees of order adsorbed onto the substrate. The layer in contact with the surface is usually highly ordered due to strong molecule–substrate interactions. Subsequent layers are more and more loosely bound (due to increasing distance from the substrate surface) and may become more and more amorphous unless the surface structure is similar to a bulk crystallization plane. In order for the STM tip to reach the current setpoint value, it pushes through many layers of loosely-organized or amorphous molecules until it reaches a well-organized layer which can transport electrons/charge well enough to support the predetermined tunneling current. There are two requirements for the imaging of multiple adsorbed layers: (1) the multiple layers must be sufficiently organized, and (2) these

organized layers must be able to support facile charge transport to the substrate. Due to the insulating nature of the majority of the molecules investigated by STM, it was thought only the molecular layer in direct contact with the surface could be imaged. Since then there have been a number of instances demonstrating that islands adsorbed upon monolayers or second layer adsorption can be observed with STM.^{2,4,65} However, there are few reports in the literature showing STM images of multiple adsorbed layers, presumably due to a lack of molecular systems which are organized over several molecular layers and also are able to transport charge easily over this distance of several molecular layers. Liquid crystalline molecules form many layers of organized molecules; however, they cannot transport electrons or charge easily through these layers. As a result, multilayers of these molecules have not yet been imaged with molecular resolution with STM.

Many molecular systems have been reported to form organized multilayers which can be resolved via AFM but not in STM images.^{59,65,66} DAPDA is one such molecule that self-organizes in three-dimensions.⁵⁹ As mentioned before, DAPDA has a dialkylamino functionality that is similar to the squaraines and forms multiple layers of ordered molecules. However, DAPDA has no D–A–D chromophore. Gorman et al. demonstrated that multiple layers of DAPDA molecules can be imaged with atomic force microscopy, but only single layers are imaged with STM.⁵⁹ The inability to image multiple layers of DAPDA with STM is most likely due to DAPDA's lack of charge-transferring functionality, precluding any charge-transfer pathway through the multiple layers of adsorbed molecules. Without a means of transporting electrons through the thickness of the multiple layers, the STM tip must push through the insulating molecular layers until it is close enough to the substrate to support the setpoint current. Thus, only the first molecular layer is imaged.

As was shown in Figure 13, squaraine multilayers can be imaged by STM. The difference between squaraine and other STM-investigated molecules, which form extensive 3D networks as a result of strong intermolecular interactions, is the inherent charge-transferring ability of squaraines in the solid state. Squaraines are exploited commercially in photoreceptors because of their charge-transporting ability. The D–A interactions between adjacent molecules within the same layer and between adjacent molecules in adjacent molecular layers provide the electronic coupling needed for facile charge transport. We have shown that additional layers of squaraines tend to adsorb such that donor and acceptor moieties within the two adjacent layers align with each other. The existence of this pathway may facilitate the imaging of several molecular layers of squaraine molecules by STM. The large gap resistance that is typically used to image squaraines (on the order of 50 gigaohms) dictates a tip–sample separation where several molecular layers can exist between the tip and the substrate. Thus tunneling can be accomplished through a great tip–substrate distance in the squaraine system due to the facile transport of electrons through the squaraine layers.

Orientation with Respect to HOPG. An important distinction was made between the alignment of the long axis of the chromophore of the molecule with the graphite lattice and the alignment of the alkyl tails of the molecule in order to determine the relationship of molecular adsorbate symmetry to graphite lattice symmetry. This

(61) Stevens, F. Thesis, University of Colorado, 1996.

(62) Ohtani, H.; Wilson, R. J.; Chiang, S.; Mate, C. M. *Phys. Rev. Lett.* **1988**, *60*, 2398.

(63) Chiang, S.; Wilson, R. J.; Mate, C. M.; Ohtani, H. *J. Microsc.* **1988**, *2*, 567.

(64) Foster, J. S.; Frommer, J. E. *Nature* **1988**, *333*, 542–544.

(65) Eng, L. M.; Fuchs, H.; Buchholz, S.; Rabe, J. P. *Ultramicroscopy* **1992**, *42–44*, 1059–1066.

(66) Schwinn, T.; Gaub, H. E.; Rabe, J. P. *Supramol. Sci.* **1994**, *1*, 85–90.

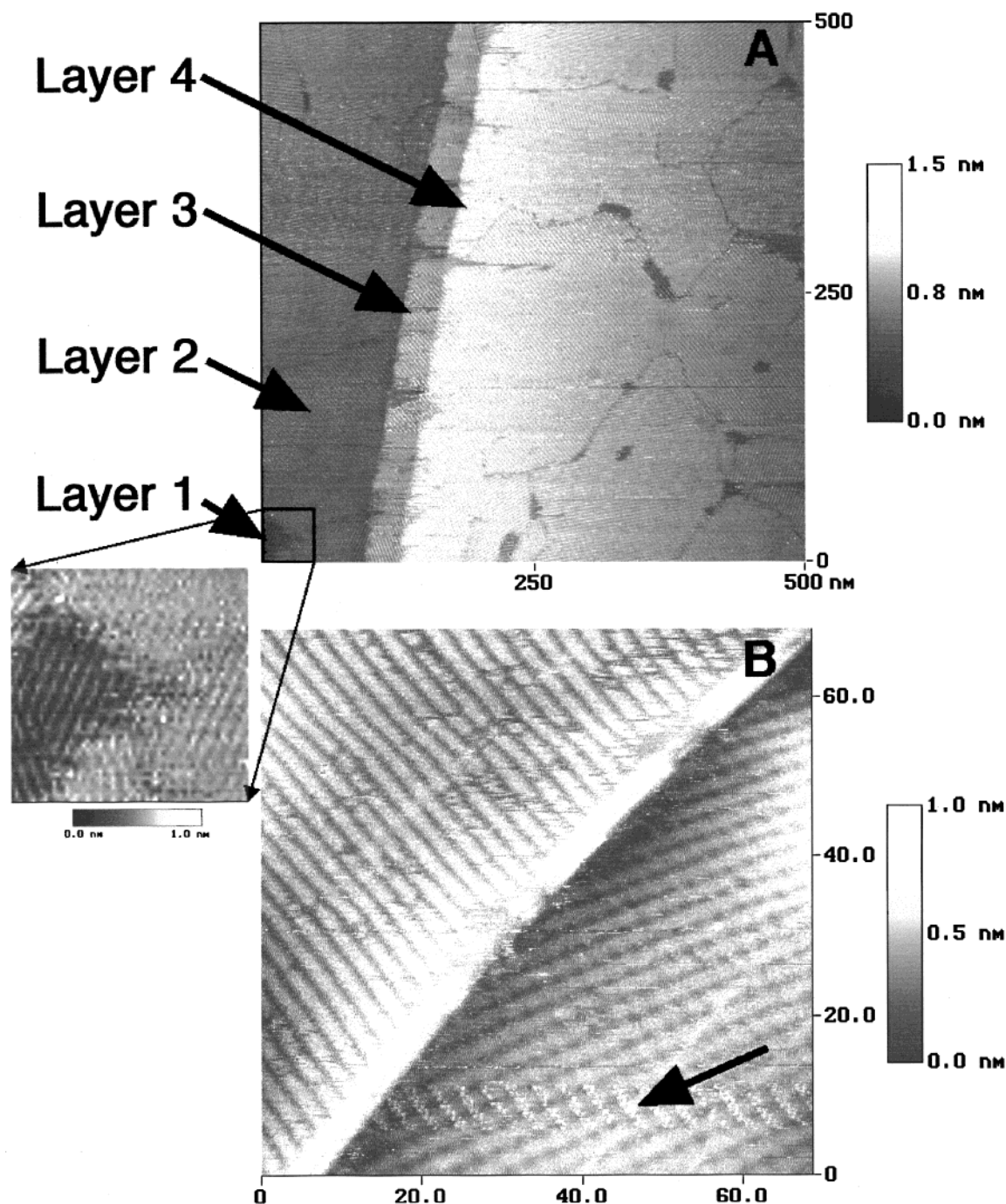


Figure 13. (A) STM image (500 nm \times 500 nm) of the ordered adsorption produced by the deposition of an 8-8/12-12 squaraine mixture (10/1 ratio) on HOPG. There are four molecular layers evident in this image (from bottom left to right), one adsorbed atop the other. The inset shows the first layer and the edge of the second in greater detail. Edges of molecular layers were measured to be 2.5 ± 0.5 Å each in height relative to one another. Overlaying of donor-acceptor moieties within adjacent layers may facilitate formation of such a multiple-layer structure through donor-acceptor charge transfer and Coulomb interactions and likewise may introduce a pathway for tunneling through these many molecular layers. To our knowledge this is the most extensive example of STM resolved multiple-layer imaging of adsorbed molecules as of yet. (B) STM image (70 nm \times 70 nm) showing the ordered adsorption of 12-12 squaraine at a graphite step edge. Contrary to step edges caused by multiple layer ordering of squaraines, adsorption at graphite step edges is always amorphous along the edge of the step. This preferential adsorption produces a thick bright stripe running parallel to the step edge. In multiple layering, squaraine rows extend all the way to the edge of the step, as in A. On the lower terrace of this image crisscrossing of multiple layers of squaraine causes a crosshatch pattern to emerge. The arrow points to the beginnings of growth of yet another layer of squaraine rows.

distinction was not previously needed for studies with linear adsorbates. Thus, these two alignments of the squaraine adsorbate must be analyzed separately. It has been shown previously that long chain alkanes preferentially align along the carbon chain or [0120] direction of the graphite lattice^{1,12} (see Figure 14A). Therefore, we might expect that the longer tails in the squaraine series

might align along this direction. It is not known how a squaraine chromophore aligns on the graphite surface. The most common polytype of graphite forms layers with the lattice vectors of two adjacent planes coinciding; however, the aromatic rings within adjacent planes do not. They are slipped by 1.42 Å, as seen in Figure 14B. We assume that a likely vector for the long axis of a

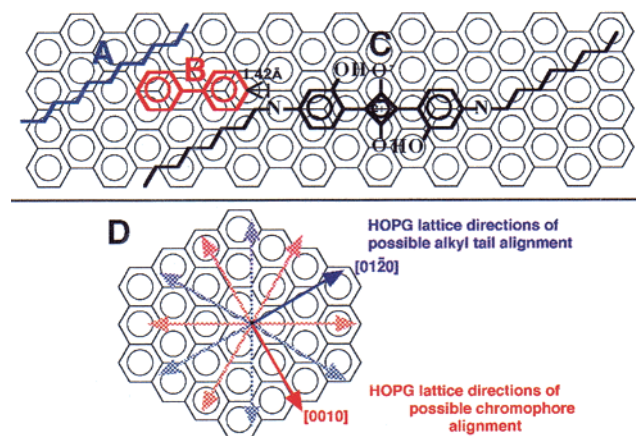


Figure 14. Cartoon showing the graphite lattice and the preferred orientation of several molecular adsorbates. (A) Preferred orientation of alkanes adsorbed on the graphite surface: aligned along the carbon chain backbone of the graphite lattice. (B) Biphenyl representing the position of a very small portion of a second graphite layer with respect to the orientation of the first layer. The directions of the lattice vectors for each of the layers coincide; however, the two are slipped relative to one another 1.42 Å along the chain of rings. (C) Theoretically expected position of the squaraine molecule oriented on the graphite lattice. The chromophore lies parallel to the same lattice direction as the biphenyl representation, and the alkyl tails lie parallel to the same lattice direction as the alkane representation. (D) Cartoon showing the graphite lattice vectors along which the squaraine chromophores and alkyl tails may be expected to align or lie parallel to. The red arrow represents one of the graphite vectors the squaraine chromophore may be expected to align along ([0010]). Other vectors symmetrically equivalent to the [0010] one are shown in muted red. The purple arrow represents one of the graphite lattice vectors the squaraine alkyl tails may be expected to align along or lie parallel to ([0120]). Symmetrically equivalent vectors are shown in muted purple.

squaraine chromophore to orient, should it be aligned, would be along the [0010] direction or symmetry-related directions (the directions of the graphite carbon chains). Aligning the squaraine chromophore along this direction would maximize π stacking between the squaraine rings and the graphite rings. Figure 14C shows a cartoon representation of our expected orientation of a squaraine molecule on the graphite surface, taking into account the alignment of both the alkyl tails and the chromophore with the graphite surface.

To determine any alignment of the squaraine layers with the graphite substrate, images of graphite were used as a reference to compare the positions of adsorbed squaraine molecules. Graphite images were obtained by increasing the setpoint current and decreasing the bias voltage in the same area where submolecularly resolved squaraine images had been obtained. The graphite lattice vectors of possible chromophore alignment and alkyl tail alignment were then determined (see Figure 14D). Images of molecularly resolved squaraines provided the directions of the long axes of the squaraine chromophores, which were then compared to the directions of the rings in the graphite lattice ([0010] and related vectors in Figure 14D). Figure 15A shows a graphical compilation of the deviation of the angle of the chromophores' long axes from the expected orientation (i.e. parallel to the [0010] or related direction in Figure 14D). Only the major polymorph of each of the five squaraines is represented in this graph.

To determine the alignment of squaraine alkyl tails, we assumed that two of the alkyl tails (4 for 2-18 SQ) adsorbed onto the surface coplanar with the chromophore

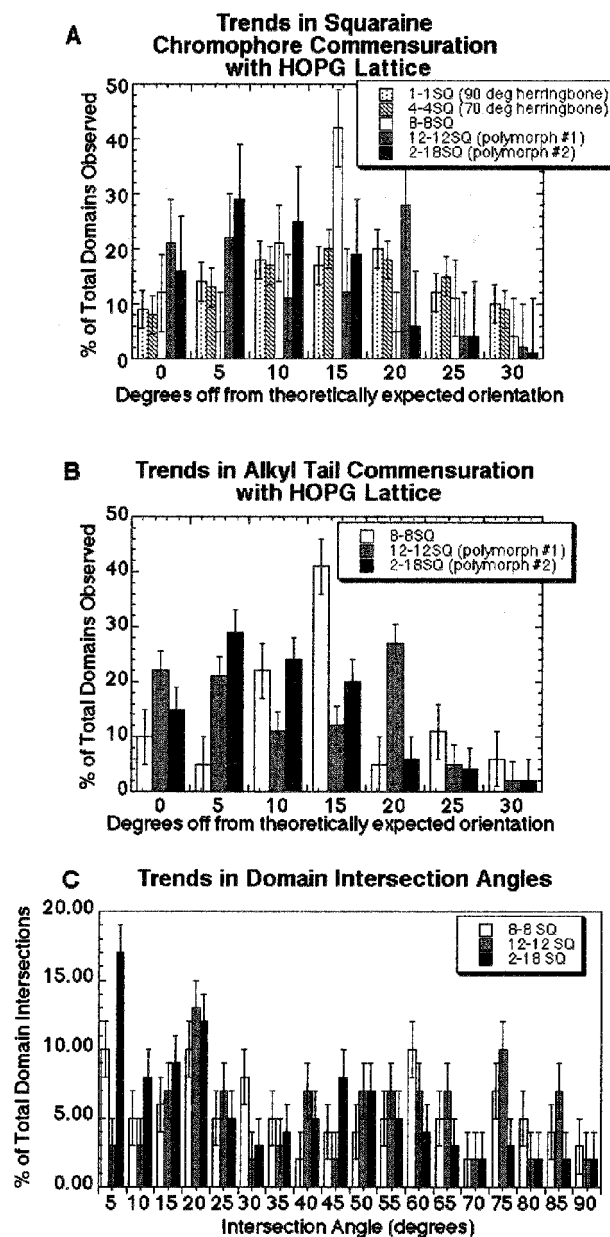


Figure 15. Histograms showing the trends in orientation of (A) the chromophores in the major polymorphs of 1-1 SQ, 4-4 SQ, 8-8 SQ, 12-12 SQ, and 2-18 SQ and (B) the alkyl tails in the major polymorphs of 8-8 SQ, 12-12 SQ, and 2-18 SQ with respect to the [0010] symmetry-related and [0120] symmetry-related graphite lattice vectors, respectively. Histogram C shows the trends in domain intersection angle for the ordered domains of adsorbed 8-8, 12-12, and 2-18 squaraine on HOPG. Molecular orientation and domain intersection angles are two of the characteristics useful in determination of the degree of commensuration of an adsorbed layer to its substrate. Here it can be seen that no squaraine polymorphs show true alignment with the graphite lattice.

and at a 30° angle to the direction of the long axis of the chromophore (as is represented in the molecular models of 8-8 SQ and 12-12 SQ). This angle of the tails to the long axis of the chromophore was determined through minimization of the molecular structure and constraining it to be coplanar using the molecular-modeling program Biograf. It was possible to deduce the orientation of the alkyl tails with respect to the graphite lattice from the determined direction of the long axis of the chromophore with respect to the graphite lattice (provided the assumption is valid). Determination of the orientation of the alkyl tails was not attempted for the shorter-tailed squaraines,

1-1 SQ and 4-4 SQ, since there is more ambiguity associated with the orientations of the tails in 1-1 SQ and 4-4 SQ than in the longer-tailed squaraines. Figure 15B shows the graphical compilation of the deviation of the assumed tail direction from the expected orientation of the 8-8, 12-12, and 2-18 squaraine tails shown in Figure 14C. The same polymorphs as those sampled for the chromophore alignment histogram are represented in the alkyl tail alignment histogram. Since the angular difference between the orientation of the chromophore and the direction of the adsorbed alkyl tail is 30°, and the angular difference between the [0010] direction and the [0120] direction is likewise 30°, the histogram for the alignment of the tails is essentially the same as the histogram for the alignment of the chromophores.

Parts A and B of Figure 15 show that the expected orientations of the squaraine chromophore and of the adsorbed alkyl tails are not preferred by any of the squaraines listed. The only significant spike in the histogram appears to be for 8-8 SQ at 15° from the expected orientation. It is not clear why this orientation is slightly preferred for 8-8 SQ. When the squaraine chromophore is rotated 15° from the expected direction, the tails should be 15° rotated from the direction of the preferred alkane chain alignment ([0120] direction). The other squaraine polymorphs apparently can accommodate any position on the graphite surface, although orientations far from the expected directions (25° and 30°) seem to be slightly disfavored among all squaraines except 1-1 SQ and 4-4 SQ. 1-1 SQ and 4-4 SQ have no preferred orientation. When the percentages of total domains oriented at the expected orientation along the [0010] and symmetry-related directions were compared among the five squaraine polymorphs listed, it was found that 12-12 SQ and 2-18 SQ exhibited the highest occurrence of domains at the expected orientation (although this orientation was not the highest occurring orientation for either of these molecules). 1-1 SQ and 4-4 SQ showed the lowest occurrence of domains at this orientation, with a very even percentage of domains across the whole range of orientations.

In addition to measuring the orientation of the individual molecules with respect to the graphite lattice, the angle formed between the directions of stripes within adjacent domains was measured and compiled for the row-forming squaraines (8-8 SQ, 12-12 SQ, and 2-18 SQ). This angle was termed the "domain intersection angle". A histogram relating the percentages of total domain intersections observed at various angles for each of the longer-tailed squaraines is shown in Figure 15C. An aligned adsorbate structure should show spikes in the intersection angle histogram at angles reflecting the symmetry of the graphite lattice (30°, 60°). No strong preference for any domain intersection angles is seen with the exception of 2-18 SQ, where there is a significant low-angle domain intersection preference at about 5°.

We conclude that none of the squaraine molecules studied form a truly aligned structure with respect to the orientation of the HOPG substrate. This result is somewhat surprising when the theoretical influence of alkyl tail length on commensuration is considered. The fact that 1-1 SQ and 4-4 SQ do not show any tendency toward alignment with the HOPG surface can be easily understood, since the donor-acceptor intermolecular charge-transfer interactions (or Coulomb forces between oppositely polarized moieties of adjacent molecules) of the squaraine core are dominant. Maximizing the donor and acceptor interaction by having adjacent molecules canted toward each other results in a herringbone pattern much

like that observed for perylenes on HOPG and MoS₂.^{67,68} Structural differences between 1-1 and 4-4 are most likely due to the steric effect of the additional 12 methylene groups in 4-4 SQ. The existence of at least three different 1-1 SQ polymorphs points to the flexibility of the structure while still maintaining strong Coulomb interactions. The observed instability of the 4-4 SQ structures may be due to an inflexibility where slight orientational changes in molecular position may interfere with the molecule-molecule forces, causing the butyl groups to eclipse favorable interactions between adjacent oppositely polarized moieties.

The increased tail length of 8-8 SQ induces a structural transition in which the herringbone-like structures of 1-1 and 4-4 SQ are now disfavored and a row structure is formed. The row structure reduces the donor-acceptor interactions of the herringbone structure. Instead, dispersion interactions between molecules in adjacent rows dominate. As a result, the molecules arrange to maximize the interdigitation of alkyl tails between adjacent rows. Reorienting the squaraine molecules from a herringbone to a row structure does not preclude donor-acceptor or Coulomb interactions between adjacent squaraine chromophores within the same row. The $65 \pm 5^\circ$ angle between the long axis of the molecules and the direction of the molecular row results in adjacent molecules within the same row being offset from each other by about 3 Å. This allows the adjacent donor and acceptor sites to interact. It appears that the interaction between the octyl tails and the HOPG substrate is not strong enough to overcome the molecule-molecule interactions between adsorbed squaraines, resulting in no alignment with the graphite lattice. Additional evidence that an eight-carbon tail is not sufficient to promote alignment is provided by an STM study of the ordered adsorption of the dialkylamine molecule DAPDA, containing two decyl groups, as reported by Gorman et al.⁵⁹ This molecule, analogous in structure to the two dialkylamino moieties of squaraines we studied, adsorbs to produce domains of linear rows that show no strong epitaxy with the HOPG surface.⁵⁹ The interaction between 14 methylenes (if two of the four tails are lying flat) and the HOPG lattice is not sufficient to overcome the molecule-molecule interactions between squaraines and promote an epitaxial structure instead.

Increasing the length of the alkyl tail to 12 carbons, as is the case for 12-12 SQ, results in the interaction between 22 methylene groups and the graphite surface. This increased interaction results in 12-12 SQ showing a slight tendency to align along the major lattice vectors of HOPG. The molecular packing within the row structure of 12-12 SQ, however, does not appear to change very much from that of 8-8 SQ, as a result of the small increase in graphite interaction. The $60 \pm 5^\circ$ angle of the chromophore of the molecule to the direction of the row ensures the interaction of the donor and acceptor moieties of adjacent molecules within the same row. It appears that even with the greater interaction of the alkyl tail with the substrate, the strength of CT interactions and Coulomb interactions between squaraine cores is important. One might expect that with 18-carbon tails the surface structure of 2-18 SQ would be commensurate due to a very large interaction between its 34 methylenes and the HOPG lattice. This is not observed, since the 2-18 SQ molecule within polymorph 2 actually shows less alignment with the HOPG lattice

(67) Ludwig, C.; Gompf, B.; Glatz, W.; Petersen, J.; Eisenmenger, W.; Mobus, M.; Zimmermann, U.; Karl, N. *J. Phys.: Condens. Matter* **1992**, *86*, 397-404.

(68) Hoshino, A.; Isoda, S.; Kurata, H.; Kobayashi, T. *J. Appl. Phys.* **1994**, *76*, 4113-4120.

than 12–18 SQ. The length of the stearyl tail in 2–18 SQ (and the reduction in total molecular bulkiness due to the two ethyl tails) results in a flexible row structure for 2–18 SQ. In addition, rows of one polytype have been seen to transform smoothly into another polytype (Figure 1C). This structural flexibility can result in undulation of the rows, demonstrating the dominance of the molecule–molecule interactions. The minimal adsorbate–substrate interaction is also manifested in the ability of these molecules to form multilayers where many of the molecules are relatively far from the surface. We have recently shown that variations of the alkyl tail chain length in a series of perylene diimides result in a transition from herringbone to row type structures between tail lengths of 12 and 18 carbons.⁶⁹ A herringbone polytype is still observed with two 18-carbon tails. In addition, the unit cell is not significantly different from the four-carbon tail, indicating that the tails protrude into the phenyloctane above the surface. The much weaker head-group interactions in this series of molecules still dominated the surface structure when the molecules were adsorbed on graphite or MoS₂ from phenyloctane.

Conclusions

The squaraine molecules that we studied form well-ordered two-dimensional surface structures that can be imaged with STM. Squaraines are highly surface active, forming domains of adsorbed molecules with a rich variety of 2D structures and polymorphs from quite dilute

solutions in phenyloctane or liquid crystal solvents. These properties are most likely due to their propensity for intermolecular donor–acceptor interactions. The 2D structures form domains of ordered molecules from tens of nanometers to a micron in size and tend not to be in registry with the HOPG substrate. A definite change in the type of adsorbate structure was observed to occur with increasing alkyl tail length. At tail lengths of one and four carbons, various polytypes of herringbone packings were observed arising from the strong D–A interactions and Coulomb forces between oppositely polarized areas of adjacent squaraine molecules. At alkyl tail lengths of eight carbons and above, despite their nonlinear molecular geometry, qualitatively similar row structures were formed with slight variations in the angle between the long axis of the chromophore and the row direction in the various polytypes. The strong intermolecular charge-transfer interactions and the charge-transport ability of the squaraine molecules allowed the most extensive STM imaging of multiple molecular layers yet reported.

Acknowledgment. The authors gratefully acknowledge Dr. P. M. Kazmaier of the Xerox Research Centre of Canada for providing the 4–4, 8–8, and 12–12 squaraine dyes and Dr. Gregg Haggquist of Lexmark for providing the 1–1 squaraine dye. Brenda Randall is thanked for her assistance as a summer REU student. The U.S. Department of Energy, Division of Chemical Sciences, is acknowledged for financial support through Contract DE-G03-96ER14625.

LA990210T

(69) Kaneda, Y.; Sampson, D. L.; Parkinson, B. A. Manuscript to be submitted.